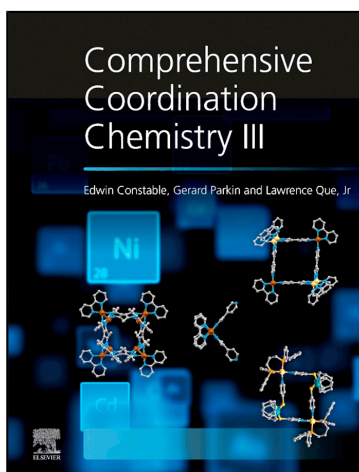


Provided for non-commercial research and educational use.
Not for reproduction, distribution or commercial use.

This chapter was originally published in *Comprehensive Coordination Chemistry III*, published by Elsevier, and the attached copy is provided by Elsevier for the author's benefit and for the benefit of the author's institution, for non-commercial research and educational use including without limitation use in instruction at your institution, sending it to specific colleagues who you know, and providing a copy to your institution's administrator.



All other uses, reproduction and distribution, including without limitation commercial reprints, selling or licensing copies or access, or posting on open internet sites, your personal or institution's website or repository, are prohibited. For exceptions, permission may be sought for such use through Elsevier's permissions site at:

<https://www.elsevier.com/about/our-business/policies/copyright/permissions>

From Hsiang, S-J.; Hayes, P. G. The Coordination Chemistry of Yttrium Complexes Supported by Multidentate Nitrogen Ancillary Ligands. In *Comprehensive Coordination Chemistry III*; Constable, E. C., Parkin, G., Que Jr, L., Eds., Vol. 4, Elsevier, 2021; pp 40–72. <https://dx.doi.org/10.1016/B978-0-12-409547-2.14922-4>
ISBN: 9780081026885

Copyright © 2021 Elsevier Ltd. All rights reserved
Elsevier

4.03 The Coordination Chemistry of Yttrium Complexes Supported by Multidentate Nitrogen Ancillary Ligands

Shou-Jen Hsiang and Paul G. Hayes, Department of Chemistry and Biochemistry, University of Lethbridge, Lethbridge, AB, Canada

© 2021 Elsevier Ltd. All rights reserved.

4.03.1	Introduction	40
4.03.1.1	Background Information	40
4.03.1.2	Scope	41
4.03.2	Synthetic Considerations	41
4.03.2.1	Salt Metathesis	41
4.03.2.2	Amine Elimination	41
4.03.2.3	Alkane Elimination	41
4.03.3	Yttrium Complexes Supported by Monoanionic Ligands	42
4.03.3.1	Monoanionic, Bidentate N,N Donors	42
4.03.3.1.1	β-Diketiminato (NacNac) ligands	42
4.03.3.1.2	Amidinate and Guanidinate ligands	44
4.03.3.1.3	Iminopyrrolyl ligands	54
4.03.3.2	Monoanionic, Tridentate N,N,N Donors	55
4.03.3.2.1	Carbazole and acridanide ligands	55
4.03.3.2.2	Tris(Pyrazoly)borate scaffolds	58
4.03.3.2.3	NNN-Pyrrole-based ligands	63
4.03.3.3	Monoanionic, Polydentate Ligands	65
4.03.3.3.1	Indolyl-containing frameworks	65
4.03.4	Dianionic Ligands	68
4.03.4.1	Dianionic, Bidentate N,N Donors	68
4.03.4.1.1	Binaphthylamido ligands	68
4.03.4.1.2	Diamide ligands	69
4.03.5	Concluding Remarks	70
References		70

4.03.1 Introduction

4.03.1.1 Background Information

Research on organometallic rare earth (lanthanides + group 3) chemistry has grown substantially during the past decade due to a dramatic increase in their application in many areas, including biological fields, as single molecule magnets and in homogenous catalysis.^{1–5} Compared to late transition metals, e.g. rhodium and palladium, rare earth elements are significantly more abundant and less expensive. Yttrium in particular has demonstrated competency for a broad range of unique stoichiometric and catalytic transformations.

Yttrium, like most rare earth metals, exists almost exclusively in the +3 oxidation state, is extremely electropositive and highly sensitive to even trace quantities of oxygen and moisture. (Very few examples of low valent rare earth metal complexes exist, and most require harsh reaction conditions/methodologies to achieve.^{6,7} Notable exceptions include Ce⁴⁺,^{8,9} Sm²⁺,¹⁰ Yb²⁺,¹⁰ Eu²⁺.^{10,11}) Synthesis of stable, well-defined organoyttrium complexes therefore requires careful ligand design that takes steric and electronic properties into account to prevent common degradation pathways such as cyclometalation, dimerization/oligomerization and ligand redistribution.¹²

Pioneering work into yttrium and group 3 coordination and organometallic compounds relied heavily on cyclopentadienyl (Cp) type donors to isolate well-behaved, monomeric, complexes.¹³ As more knowledge and understanding of the chemical behavior of these systems was garnered, research efforts began focusing upon the development of new ligand systems beyond the Cp paradigm, capable of stabilizing a wide array of yttrium species. In order to limit the aforementioned degradation pathways, multi-coordinate ligand systems that incorporate one or more “hard” nitrogen donors have become particularly prevalent. Specifically, great progress has been made generating complexes supported by monoanionic and neutral nitrogen ligands that leave more than one valence for subsequent chemistry. Complexes of some of these frameworks have proven to be highly active and selective catalysts for numerous useful and unusual chemical reactions.

This past decade in particular has seen an exponential increase in the development of new nitrogen-containing ligands for use with yttrium. In addition, a great deal of work has been conducted to expand upon previously disclosed ligand architectures. Accordingly, the current body of literature is sufficient that a comprehensive review of the coordination chemistry of yttrium complexes supported by nitrogen ligands is now warranted.

4.03.1.2 Scope

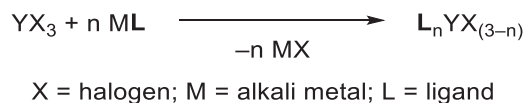
As the coordination chemistry of yttrium has been comprehensively surveyed in previous editions of this book¹⁴ and other articles,^{2,12,15,16} this contribution will encompass only new developments published within the past decade. Similarly, since cyclopentadienyl (Cp) and Cp-derived ligands constitute a large field on their own,^{13,17} they have been largely excluded. Instead, this article will focus exclusively on yttrium complexes supported by multidentate nitrogen ligands, and is organized by ligand charge (dianionic, monoanionic), as well as denticity. In acknowledging the many contributions to this field, and in the interest of brevity, we were occasionally forced to limit discussion to examples that best highlight specific structures and reactivity patterns.

4.03.2 Synthetic Considerations

Yttrium complexes are highly air and moisture sensitive, and thus, their synthesis, manipulation and storage generally requires stringent inert atmosphere techniques.¹⁸ In addition, many are thermally sensitive, especially in the solution state and when stored for prolonged periods. Accordingly, subambient temperatures are often necessary. Although routine methods for attaching anionic ligands to yttrium are well known,¹² challenges associated with this vital process remain. As these procedures are highly relevant to the chemistry discussed in this article, a brief summary has been included below.

4.03.2.1 Salt Metathesis

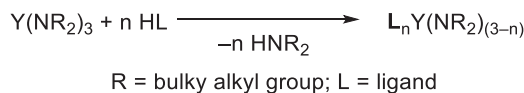
One of the most important reactions in coordination chemistry is that between alkali metal salts of ligands and metal halides (**Scheme 1**). This ligand attachment protocol is versatile and has the advantage that the salt byproduct is generally insoluble in common organic solvents, and can therefore be readily removed by filtration. In addition, the resultant yttrium complexes retain halide ligands which can prove valuable for installation of other functionalities.



Scheme 1 Generic salt metathesis reaction between yttrium trihalides and an alkali metal ligand sSalt.

4.03.2.2 Amine Elimination

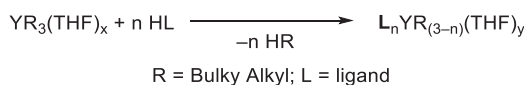
Amine elimination has proven to be a robust ligand attachment protocol for yttrium, particularly when a metal amide is sought. This straightforward process involves reaction of a proteo ligand with an appropriate yttrium amide starting material, such as the homoleptic complex $\text{Y}[\text{N}(\text{SiMe}_3)_2]_3$. The amine byproduct (HNR_2) that is eliminated can usually be removed by exposure to reduced pressure (**Scheme 2**).



Scheme 2 Generic method for installing an ancillary ligand by amine elimination.

4.03.2.3 Alkane Elimination

Perhaps the most common ligand attachment methodology used with yttrium is alkane elimination. The alkane elimination pathway follows the same principles as amine elimination and utilizes yttrium compounds that feature bulky alkyl groups, such as $-\text{CH}_2\text{SiMe}_3$, $-\text{CH}_2\text{SiMe}_2\text{Ph}$, $-\text{CH}(\text{SiMe}_3)_2$ and $-\text{CH}_2\text{Ph}$. The extruded alkane is always highly volatile, and thus, removal in vacuo is trivial. While this is an appealing pathway because one can directly obtain organometallic species, the yttrium alkyl starting materials are notoriously difficult to prepare and often decompose rapidly at ambient temperature.¹⁹ As a consequence, it is common to generate and use the yttrium trialkyl compounds in situ (**Scheme 3**).



Scheme 3 Generic route for installing an ancillary ligand by an alkane elimination protocol.

4.03.3 Yttrium Complexes Supported by Monoanionic Ligands

4.03.3.1 Monoanionic, Bidentate N,N Donors

4.03.3.1.1 β -Diketiminato (NacNac) ligands

β -Diketiminato or "NacNac" ligands are widely used to stabilize metals of varying oxidation states and coordination numbers.²⁰ The steric bulk of the ligand backbone can be fine-tuned by incorporating different substituents, with methyl and *tert*butyl (^tBu) groups being common on the 2 and 4 carbons while sterically demanding aromatics, such as 2,6-ⁱPr₂C₆H₃ are frequently installed as substituents on nitrogen (Fig. 1).

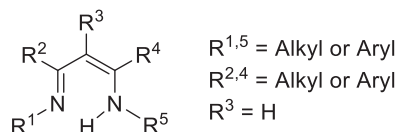
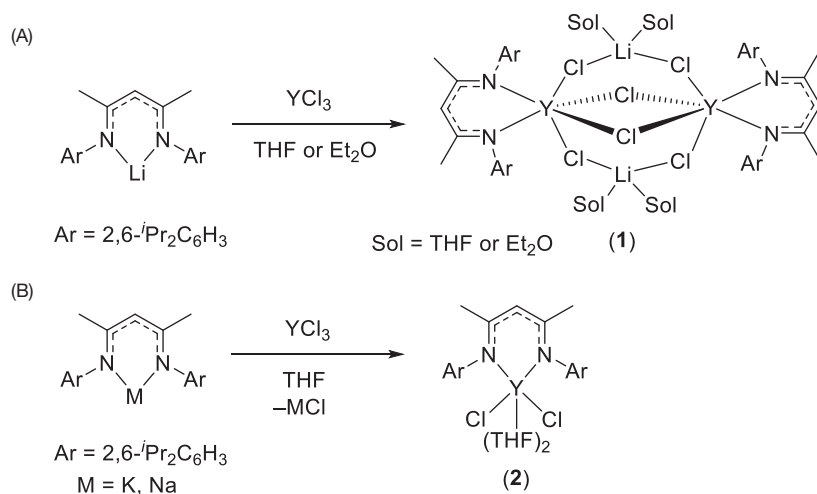


Fig. 1 Generic structure of β -diketiminato scaffold.

Synthesis of β -diketiminato yttrium complexes can be achieved by first generating the alkali metal ligand salt followed by a salt metathesis reaction with yttrium halide starting materials.^{16,21–24} Reported by Lappert et al. in 2008, when the ligand lithium salt was utilized in coordinating solvents such as tetrahydrofuran (THF) or Et₂O the dimeric structure [Y(μ -Cl){N(2,6-ⁱPr₂C₆H₃)CMe₂CH}{(μ -Cl)Li(sol)₂(μ -Cl)}₂, sol = THF or Et₂O, (1), which contains bridging chloride groups, was isolated (Scheme 4A). When the heavier alkali metals salts NaL or KL were employed, the monomeric complex [L^{Me}YCl₂(THF)₂], (2), L^{Me} = [(2,6-ⁱPrC₆H₃)NC(CH₃)CH(CH₃)N(2,6-ⁱPrC₆H₃)], was generated exclusively (Scheme 4B).²³

Piers has also reported that increasing the steric bulk of the substituents on the 2 and 4 carbons discourages solvent coordination and improves the stability of corresponding organoyttrium species (3a: L^{Me}YI₂(THF)); 3b: [L^{tBu}YI₂], L^{tBu} = [(2,6-ⁱPrC₆H₃)NC(^tBu)

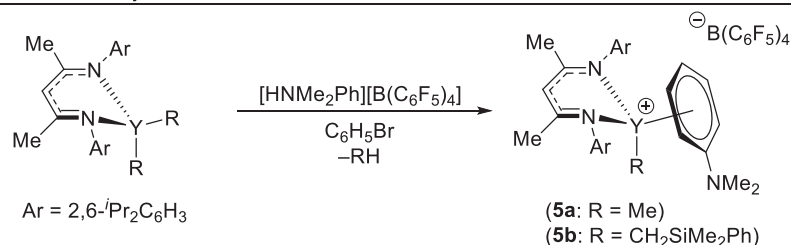
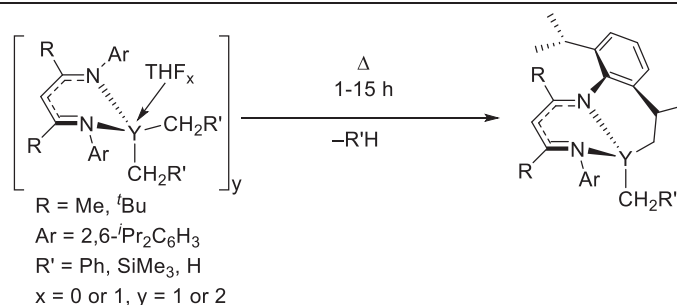
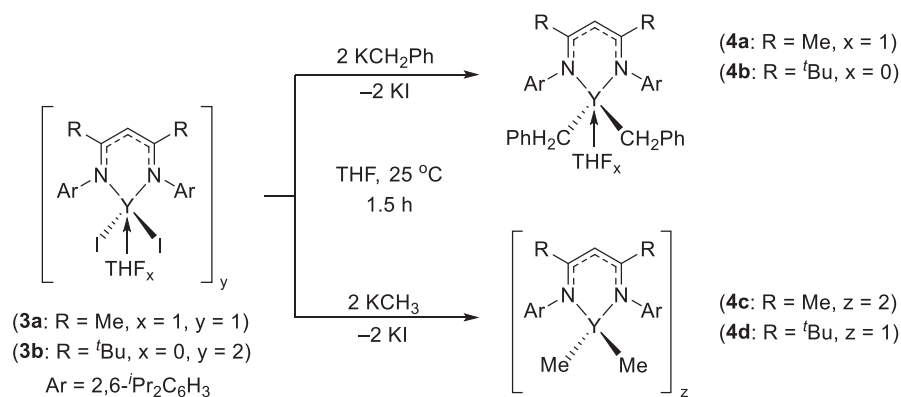


Scheme 4 Synthesis of (A) dimeric; and (B) monomeric yttrium chloride complexes.

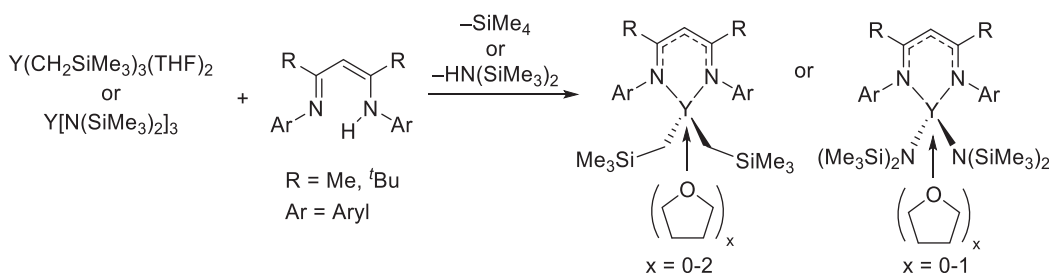
CH(^tBu)N(2,6-ⁱPrC₆H₃)] and dialkyl ((4a: L^{Me}Y(CH₂Ph)₂(THF); 4b: L^{tBu}Y(CH₂Ph)₂; 4c: [L^{Me}YMe₂]₂; 4d: L^{tBu}YMe₂) (Scheme 5, top).^{21,24} Nonetheless, even the most bulky variants were prone to loss of RH *via* cyclometalation of an aryl isopropyl moiety (Scheme 5, middle). Notably, reaction of L^{Me}YR₂ with [HNMe₂Ph][B(C₆F₅)₄] generated the organoyttrium complexes [L^{Me}YR(η^6 -NMe₂Ph)][B(C₆F₅)₄], (5a: R = Me), (5b: R = CH₂SiMe₂Ph), that featured a dimethylaniline group bound to yttrium in an η^6 fashion *via* the phenyl ring (Scheme 5, bottom). Remarkably, these cations exhibited greater thermal stability than their neutral counterparts, but intriguingly, attempts to prepare analogous cations using the L^{tBu} ligand were unsuccessful.

Synthesis of dialkyl and diamido complexes directly from Y(CH₂SiMe₃)₃(THF)₂, and Y[N(SiMe₃)₂]₃ *via* elimination reactions with proteo ligands has also been reported (Scheme 6).^{2,16,25}

The most recent reports in β -diketiminato yttrium chemistry have primarily focused on their use as catalysts for the polymerization of dienes, substituted alkenes and lactones. For instance, the C_{2v} symmetry of the most commonly used NacNac variants have allowed for appreciable *isoselective* control in the polymerization of *cis*-1,4-isoprene, thereby generating highly uniform plastics. Specifically, Cui et al. have demonstrated that the yttrium dichloride [{N(2,6-Me₂C₆H₃)CMe₂CH}YCl₂(THF)₂], (6), and dinuclear [{2,6-Me₂C₆H₃NC(Me)C(H)C(Me)N}₂(-*m*-C₆H₄)-]Y(CH₂SiMe₃)₂(THF)₂], (7), complexes can both catalyze the formation



Scheme 5 Top: Synthesis of dialkyl yttrium nacnac complexes (4a–d) starting from diiodide complexes (3a,b), Middle: decomposition of dialkyl yttrium nacnac complexes via cyclometalation, bottom: generation of cationic complexes (5a,b).

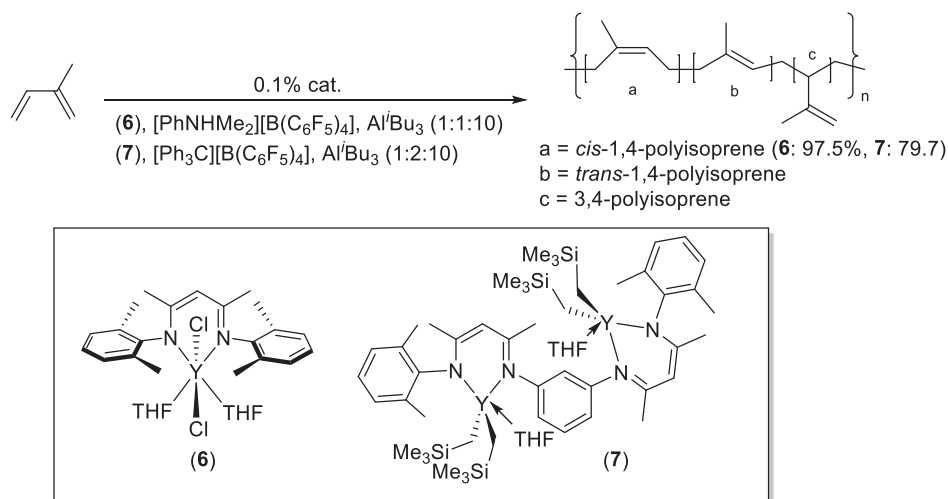


Scheme 6 Synthesis of dialkyl and diamido yttrium nacnac complexes using alkane and amine elimination pathways.

of largely *cis*-1,4-polyisoprene (97.5% and 79.7%, respectively) in a short period of time (< 10 min) under mild reaction conditions ($10\text{--}20^\circ\text{C}$, Tol).^{26,27} It is important to note that in these cases, Lewis/Bronsted acid and alkane co-catalysts were utilized to generate more active yttrium cations *in situ* (Scheme 7).

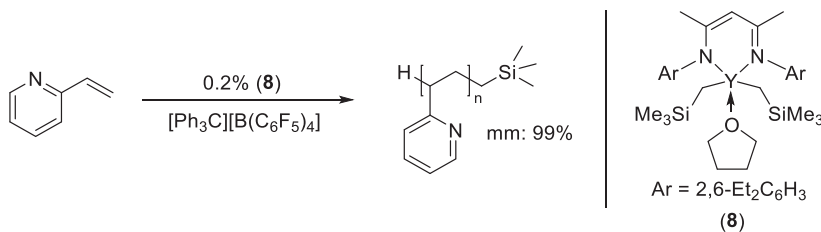
The same group has also investigated the viability of cationic organoyttrium NaCNac species to mediate the polymerization of 2-vinylpyridine.²⁸ Upon *in situ* activation of the dialkyl complex $[\{(\text{N}(2,6\text{-Et}_2\text{C}_6\text{H}_3)\text{CMe})_2\text{CH}\}\text{Y}(\text{CH}_2\text{SiMe}_3)_2(\text{THF})]$, (8), with $[\text{Ph}_3\text{C}][\text{B}(\text{C}_6\text{F}_5)_4]$, the resultant alkylyttrium cation proved to polymerize 2-vinylpyridine with near perfect tacticity (mm: 99%, Scheme 8).²⁸

Shen and co-workers have explored the use of bis(β -diketiminato) yttrium complexes as single site initiators for the polymerization of the cyclic esters *L*-Lactide (*L*-LA), ϵ -caprolactone (ϵ -CL) and methyl methacrylate (MMA).²⁹ The tested initiators, $[\{(\text{NArCMe})_2\text{CH}\}\text{Y}(\text{BH}_4)]$, (9a: $\text{Ar} = 2\text{-MeC}_6\text{H}_4$; 9b: $\text{Ar} = \text{Ph}, 2,6\text{-}i\text{Pr}_2\text{C}_6\text{H}_3$), were generated by reaction of NaBH_4 with



Scheme 7 Stereoselective polymerization of isoprene catalyzed by complexes (6) and (7).

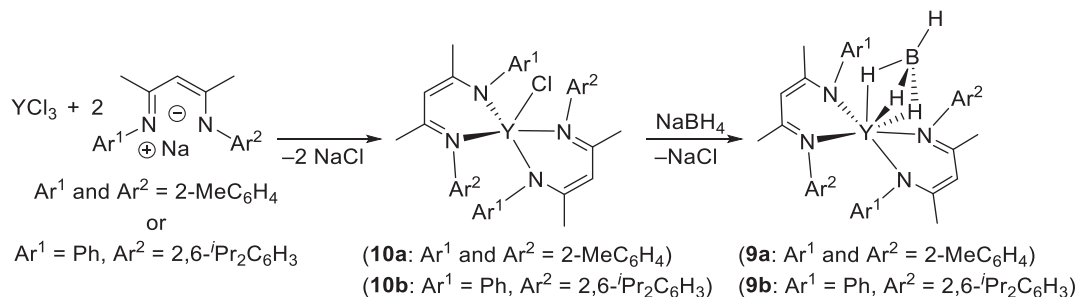
$\{[(\text{NArCMe})_2\text{CH}]\text{YCl}\}$, (10a: Ar = 2-MeC₆H₄; 10b: Ar = Ph, 2,6-*i*Pr₂C₆H₃), which in turn were prepared *via* the addition of 2 equivalents of Na $[(\text{NArCMe})_2\text{CH}]$ to YCl₃ (Scheme 9). The yttrium borohydride complexes (10a, b) produced poly-L-LA and polycaprolactone with relatively narrow molecular mass distributions ($M_w/M_n = 1.35\text{--}1.48$) and high yields (93–99%) in 3–4 min with catalyst loadings of 0.1%.



Scheme 8 Isotactic polymerization of 2-vinylpyridine by complex (8).

4.03.3.1.2 Amidinate and Guanidinate ligands

Amidates were one of the first alternatives to Cp ligands that were used to stabilize group 3 metal complexes.³⁰ The steric and electronic properties of these scaffolds can be readily adjusted by modifying the substituents on the central carbon and/or two nitrogen atoms (Fig. 2A). As a consequence, a wide array of coordination modes and geometries have been observed. Guanidinate ligands are closely related to amidinates, with the only difference being an NR₂ group attached to the central carbon (Fig. 2B). Similar flexibility in ligand structure and electronics have been achieved with guanidinate ligands, but the additional amine provides another location to fine-tune the properties of these systems.³¹ Both amidinate and guanidinate ligands typically bind in a bidentate κ^2 manner; however, closely related linked derivatives, and versions that bear a pendant donor, exhibit bonding modes with increased denticity (Fig. 2C and D).



Scheme 9 Synthesis of Bis(NacNac) yttrium complexes and subsequent derivatization to form borohydride complexes (9a,b).

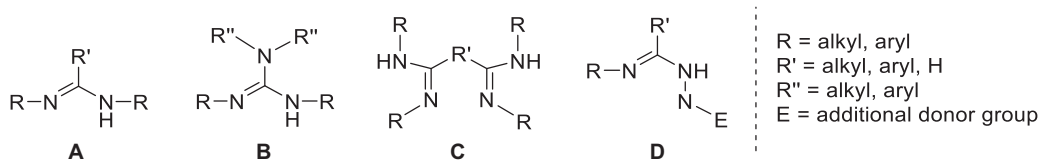


Fig. 2 Generic structures of (A) amidinates; (B) guanidates; (C) linked bis(amidinates); and (D) functionalized amidinates.

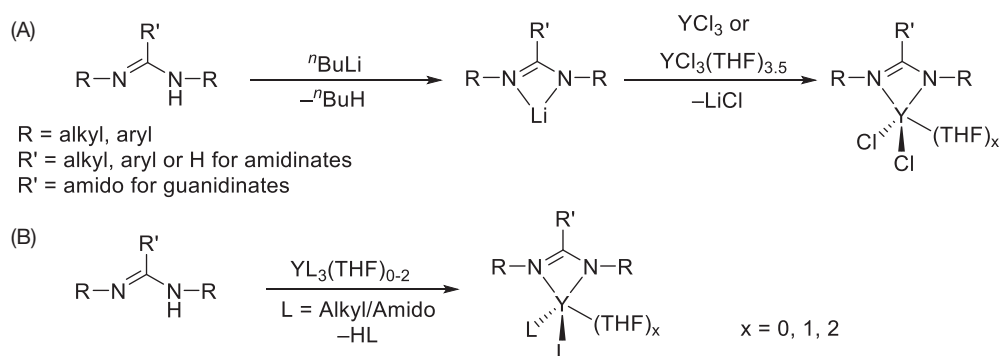
Addition of amidinate and guanidinate ligands to yttrium most commonly proceeds through a salt metathesis reaction between the lithium salt of the ligand and an yttrium trichloride starting material (**Scheme 10A**).¹⁶ Elimination routes to amidinate and guanidinate supported yttrium species have also been reported (**Scheme 10B**).^{32,33}

A novel synthetic procedure involving the construction of an amidinate ligand at yttrium was demonstrated by the Tsurugi group.³⁴ In this instance, amidinate complexes [$\{(2,6\text{-}i\text{Pr}_2\text{C}_6\text{H}_3)\text{NCH}=\text{CHN}(2,6\text{-}i\text{Pr}_2\text{C}_6\text{H}_3)\text{Y}\{(\text{N}(\text{C}_6\text{H}_{11}))_2\text{CC}\equiv\text{CR}\}(\text{THF})\}$] (**11a**: R = SiMe₃; **11b**: R = ⁿPr) and [$\{(2,6\text{-}i\text{Pr}_2\text{C}_6\text{H}_3)\text{NCH}=\text{CHN}(2,6\text{-}i\text{Pr}_2\text{C}_6\text{H}_3)\text{Y}\{(\text{N}(\text{C}_6\text{H}_{11}))_2\text{CCR}=\text{C}=\text{CH}_2\}(\text{THF})\}$] (**11c**: R = ⁿPr; **11d**: R = Ph) were generated by insertion of *N,N'*-dicyclohexylcarbodiimide into yttrium η^3 -propargyl/allenyl moieties (**Scheme 11**).

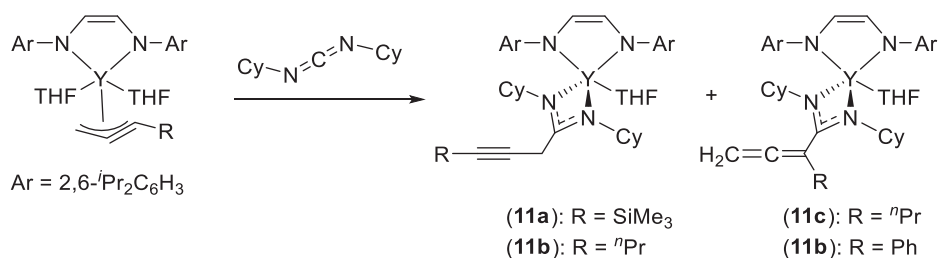
Bochkarev and co-workers have highlighted the versatility in coordination modes of amidinate ligands through the synthesis of the dinuclear complex [$\{[\text{MeNC}(\text{Me})\text{NMe}]_2\text{Y}\}_2[\mu\text{-}\eta^2:\eta^2\text{-MeNC}(\text{Me})\text{NMe}]_2$], (**12**) (**Scheme 12**); which contains both terminal and bridging amidinate ligands.³⁵ The nitrogen atoms of the bridging amidinate coordinate to both metal centers *via* an unusual $\mu\text{-}\eta^2:\eta^2$ motif, rather than the expected $\mu\text{-}\eta^1:\eta^1$.

Hessen et al. were able to catalyze the hydrosilylation of terminal alkenes using mono(guanidinate) and mono(amidinate) yttrium dialkyl complexes [$\{((2,6\text{-}i\text{Pr}_2\text{C}_6\text{H}_3)\text{N})_2\text{C}(\text{NMe}_2)\text{Y}(\text{CH}_2\text{SiMe}_3)_2(\text{THF})\}$], (**13**) and [$\{((2,6\text{-}i\text{Pr}_2\text{C}_6\text{H}_3)\text{N})_2\text{CPh}\text{Y}(\text{CH}_2\text{SiMe}_3)_2(\text{THF})\}$], (**14**) (**Scheme 13**).³² These catalysts showed complete selectivity for the anti-Markovnikov product when simple alkyl substrates were employed. In addition, they exhibited reasonable activity with conventionally challenging substrates, such as Lewis basic acetal or 1,3-dithianine. Comparisons between the amidinate and guanidinate species with substrates that possess additional donor groups such as 4,4-diethoxybut-1-ene, revealed that the metal center of the guanidinate complex was less electrophilic than that of the amidinate analogue. This is postulated to be due to the disparity in selectivity between the two complexes as metal affinity for the ether functionality would promote selectivity for the Markovnikov product (*vide infra*). Crystallographic data revealed elongated Y–C bond lengths, while ¹H NMR spectroscopy revealed an upfield shift in the Y–CH₂ resonance for the guanidinate species compared to the amidinate.

Complex (**14**), upon sequential reaction with [HNMe₂][BPh₄] and 10 atm of H₂, afforded the rare cationic terminal yttrium hydride [$\{((2,6\text{-}i\text{Pr}_2\text{C}_6\text{H}_3)\text{N})_2\text{CPh}\text{YH}(\text{THF})_3\}[\text{BPh}_4]$], (**15**), which reversibly dimerizes to form [$\{((2,6\text{-}i\text{Pr}_2\text{C}_6\text{H}_3)\text{N})_2\text{CPh}\}$]

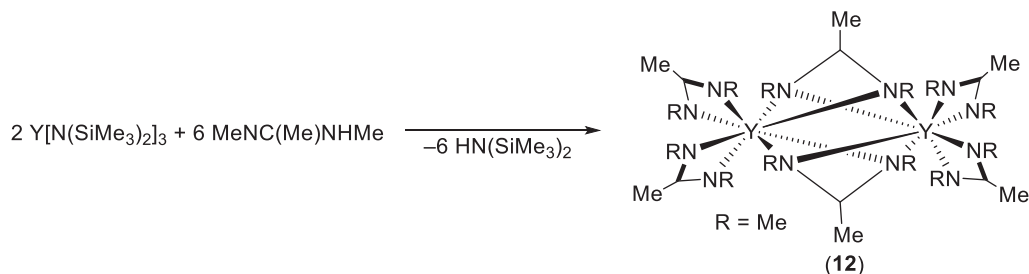


Scheme 10 General synthetic routes to amidinate and guanidinate yttrium complexes.



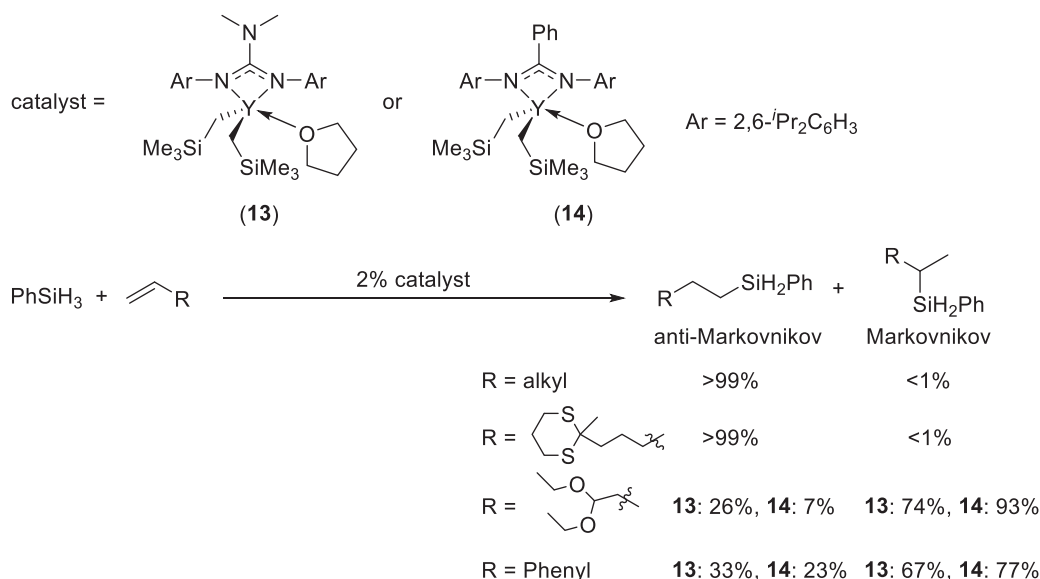
Scheme 11 Construction of amidinate ligands at yttrium.

$\text{Y}(\text{THF})_2(\mu\text{-H})_2[\text{BPh}_4]$ (**16**) (Scheme 14).³⁶ While the reactivity of these species were not explicitly investigated, the lutetium analogue of (**15**) reacts with *N,N'*-diisopropylcarbodiimide to give the expected cationic formamidinate complex $[\text{Lu}\{\{(2,6\text{-}i\text{Pr}_2\text{C}_6\text{H}_3)\text{N}\}_2\text{C}(\text{Ph})\}\{\text{PrN}(\text{CH})\text{N}^i\text{Pr}\}(\text{THF})_2][\text{BPh}_4]$.



Scheme 12 An example of an yttrium complex (**12**) with both terminal and bridging amidinate ligands.

Formamidinate ligands that lack substituents on the central carbon have thus far only been substantially investigated by the Anwander group.^{37,38} The tetramethylaluminate complex $[\{(2,6\text{-}i\text{Pr}_2\text{C}_6\text{H}_3)\text{N}\}_2\text{CH}\}\text{Y}(\text{AlMe}_4)_2]$, (**17**), readily catalyzes the polymerization of isoprene, but the stereoselectivity of the resultant polymer is dependent upon the co-catalyst.³⁷ When the Lewis acid $[\text{Ph}_3\text{C}][\text{B}(\text{C}_6\text{F}_5)_4]$ was employed, up to 84% 1,4-*trans*-selectivity was observed. Conversely, when the Brønsted acid activator $[\text{PhNMe}_2\text{H}][\text{B}(\text{C}_6\text{F}_5)_4]$ was used, moderate *cis*-1,4-selectivity (58.2%) prevailed. Addition of one equivalent of AlMe_3 to the Brønsted acid system increased 1,4-*trans*-selectivity slightly (13–45%) (Scheme 15).



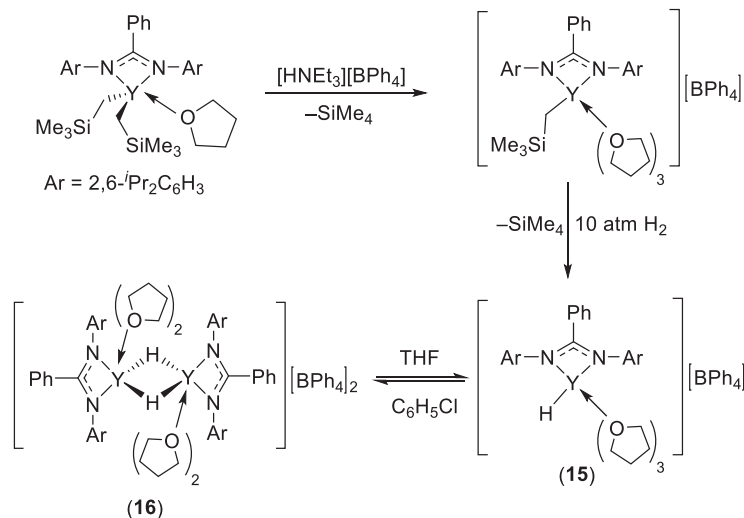
Scheme 13 Hydrosilylation of terminal alkenes catalyzed by complexes (**13**) and (**14**).

As with the previously mentioned NacNac species, amidinate and guanidinate yttrium complexes have exhibited competence as catalysts for the polymerization of isoprene and lactide (Fig. 3).^{39,40}

While no activity was observed for either $[\{(2,6\text{-}\text{Me}_2\text{C}_6\text{H}_3)\text{N}\}_2\text{C}(\text{C}_6\text{H}_{11})\}\text{Y}(\text{N}(\text{SiMe}_3)_2)_2]$, (**18a**), or $[\{(2,6\text{-}\text{Me}_2\text{C}_6\text{H}_3)\text{N}\}_2\text{CPh}\}\text{Y}(\text{N}(\text{SiMe}_3)_2)_2]$, (**18b**), in the absence of a co-catalyst, addition of $[\text{Ph}_3\text{C}][\text{B}(\text{C}_6\text{F}_5)_4]$ and AlMe_3 yielded highly active systems for isoprene polymerization even at -10°C in toluene.³⁹ In fact, complete conversion to an almost exclusively (94.5%) *cis*-1,4 selective polymer was observed after only 2 min at a 0.2% loading of complex (**18a**) at 25°C .³⁹

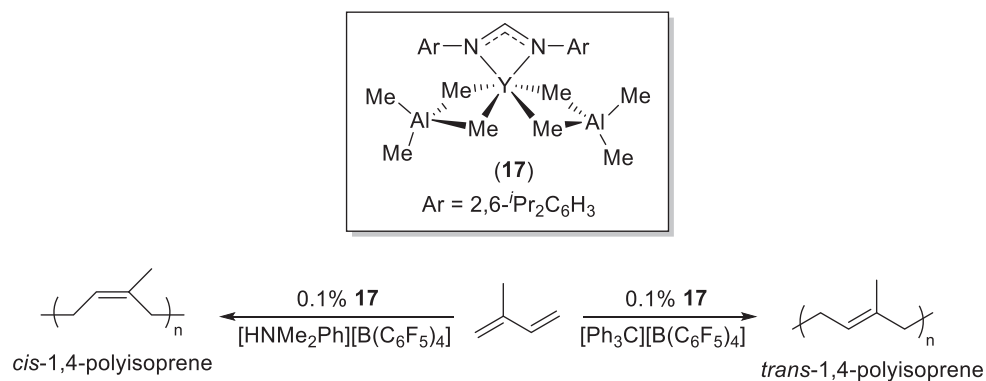
The related guanidinate complexes $[\{(2,6\text{-}\text{Me}_2\text{C}_6\text{H}_3)\text{N}\}_2\text{C}(\text{N}(\text{SiMe}_3)_2)\}\text{Y}(\text{N}(\text{SiMe}_3)_2)_2]$, (**19a**), and $[\{(2,6\text{-}\text{Me}_2\text{C}_6\text{H}_3)\text{N}\}_2\text{C}(\text{N}(\text{SiHMe}_2)_2)\}\text{Y}(\text{N}(\text{SiHMe}_2)_2)_2]$, (**19b**), were investigated as catalysts for the ROP of *rac*-lactide and *l*-lactide.⁴⁰ Complex (**19b**) exhibited remarkable activity for the ROP of *l*-lactide, boasting a 93% conversion after 2 min at 50°C , with the high $[\text{lactide}]:[\text{catalyst}]$ ratio of 10,000:1. Intriguingly, complex (**19b**) was significantly less active and displayed mediocre tacticity control when *rac*-lactide was used (88% conversion after 1 h at 25°C with a 4000:1 lactide:catalyst ratio) (Table 1).⁴⁰

The bis(aminobenzyl) yttrium amidinate complex $[\{(2,6\text{-}i\text{Pr}_2\text{C}_6\text{H}_3)\text{N}\}_2\text{CPh}\}\text{Y}(o\text{-CH}_2\text{C}_6\text{H}_4\text{NMe}_2)_2]$, (**20**), first reported by Hou, is another example of an organoyttrium complex, which upon activation with $[\text{Ph}_3\text{C}][\text{B}(\text{C}_6\text{F}_5)_4]$, catalyzes the polymerization of isoprene in a regio- and stereoselective fashion.³³ Specifically, it was reported that this system quantitatively consumes 750 equivalents of isoprene in 2 min at ambient temperature, affording polyisoprene with high 3,4-regioselectivity (91%) and moderate isotacticity



Scheme 14 Synthesis of amidinate-supported cationic hydride complexes (**15**) and (**16**).

($mm = 50\%$). Even better regio- and stereoselectivity were achieved when the polymerization was carried out at temperatures less than -10°C (3,4-selectivity up to 99.5%, $mmmm$ up to 99%). Significantly, the addition of >5 equivalents of AlMe_3 to the **20**/ $[\text{Ph}_3\text{C}][\text{B}(\text{C}_6\text{F}_5)_4]$ mixture completely reversed the regioselectivity in favor of 1,4-*cis*-polyisoprene (98% at -10°C) (**Scheme 16**).



Scheme 15 Co-catalyst dependence in the regioselective polymerization of isoprene.

This phenomenon was postulated to be due to the formation of a tetramethylaluminate complex $[\text{Y}\{(2,6\text{-}i\text{Pr}_2\text{C}_6\text{H}_3)\text{N}\}_2\text{C}(\text{Ph})\}\{\text{AlMe}_4\}_2]$ analogous to (**17**) (*vide supra*), which also requires activation with $[\text{Ph}_3\text{C}][\text{B}(\text{C}_6\text{F}_5)_4]$. The isoprene can

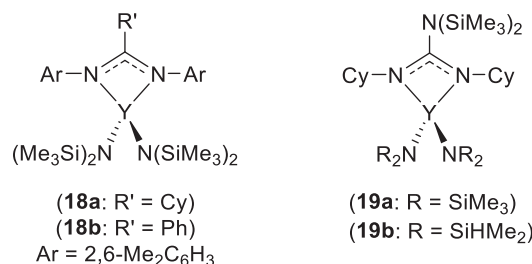


Fig. 3 Monoamidinate and guanidinate yttrium complexes used by the Luo group.

supposedly coordinate to both yttrium and aluminum while in the *cis* conformation, which apparently results in a reversal of regioselectivity (Scheme 17).

Interestingly, when only 2 equivalents of AlMe_3 was added to complex (20), a mixed methyl/methylidene cluster, $[\text{Y}_3\{((2,6\text{-}i\text{-Pr}_2\text{C}_6\text{H}_3)\text{N})_2\text{CPh}\}_3(\mu_2\text{-Me})_3(\mu_3\text{-Me})(\mu_3\text{-CH}_2)]$, (21), was generated (Scheme 18).⁴¹

Complex (21) activates various small molecules, including terminal nitrile and alkynes, as well as CS_2 , to form an array of tri-metallic clusters (22a-d).⁴¹ Notably, the reaction between (21) and phenylacetylene afforded $[\text{Y}_3\{((2,6\text{-}i\text{-Pr}_2\text{C}_6\text{H}_3)\text{N})_2\text{CPh}\}_3(\mu_2\text{-Me})_3(\mu_3\text{-Me})(\mu_3\text{-}\eta^3\text{:}\eta^1\text{-PhCCMe})]$, (22b), which features the dianionic *cis*-1-phenyl-1-propenyl moiety bound in a $\mu_3\text{-}\eta^3\text{:}\eta^1$ bonding mode (Scheme 19).

Zhou et al. have also recognized the promise that amidinate-supported yttrium species hold as catalysts for the polymerization of dienes.^{42,43} Like Hou and co-workers (*vide supra*), regioselectivity was found to be dependent upon the presence or absence of AlMe_3 . This prompted investigations into whether regioselectivity could be controlled in situ to form regioblock co-polymers

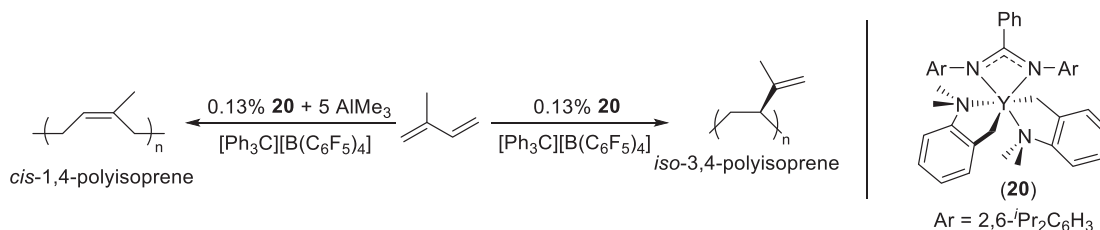
Table 1 Comparison of catalyst performance for the polymerization of isoprene.

Cat.	Co-cat. ^a	[Cat]:[AlR ₃]:[Borate]	Solvent	T (°C)	TOF/h ^{-1b}	Cis-1,4	3,4	Trans-1,4	M _w /M _n
(17)	A	1:0:1	Toluene	25	42	53.6	30.5	15.9	2.05
(17)	A / AlMe_3	1:1:1	Toluene	25	42	5.2	7.8	87.0	1.53
(18a)	B / AlMe_3	1:5:1	Toluene	25	24,000	92.5	–	–	2.44
(18b)	B / AlMe_3	1:5:1	Toluene	25	6000	91.9	–	–	2.01
(20)	B	1:0:1	$\text{C}_6\text{H}_5\text{Cl}$	25	22,500	9	91	0	1.3
(20)	B / AlMe_3	1:5:1	$\text{C}_6\text{H}_5\text{Cl}$	25	4500	91	3	6	1.6

^aA: $[\text{HNMe}_2\text{Ph}][\text{B}(\text{C}_6\text{F}_5)_4]$, B: $[\text{Ph}_3\text{C}][\text{B}(\text{C}_6\text{F}_5)_4]$.

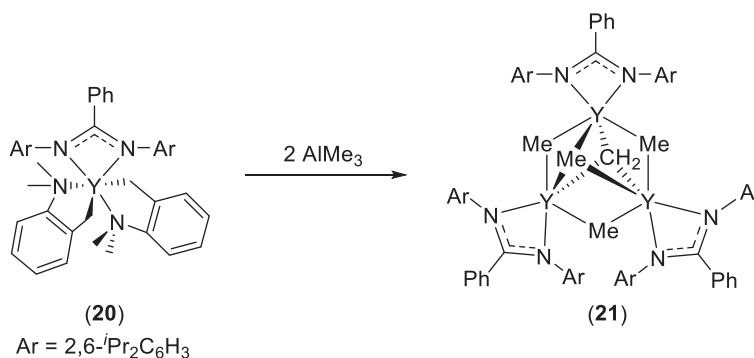
^bCalculated based on provided literature values.

of isoprene and myrcene.⁴² Experiments revealed that diblock polyisoprene could be afforded when a chlorobenzene solution of isoprene was treated with a mixture of complex (20) and co-catalysts $[\text{Ph}_3\text{C}][\text{B}(\text{C}_6\text{F}_5)_4]$ and Al^iBu_3 , followed later by 7 equivalents of AlMe_3 , and finally, another aliquot of isoprene (Scheme 19A). Al^iBu_3 was identified as essential to forming diblock polyisoprene and postulated to be both a stabilization and chain transfer agent.⁴² A similar strategy proved successful for preparing diblock (3,4- and 1,4-*cis*-) polymers of β -myrcene (Scheme 19B). Finally, regioselective copolymerization of isoprene and myrcene was demonstrated (Scheme 19C).



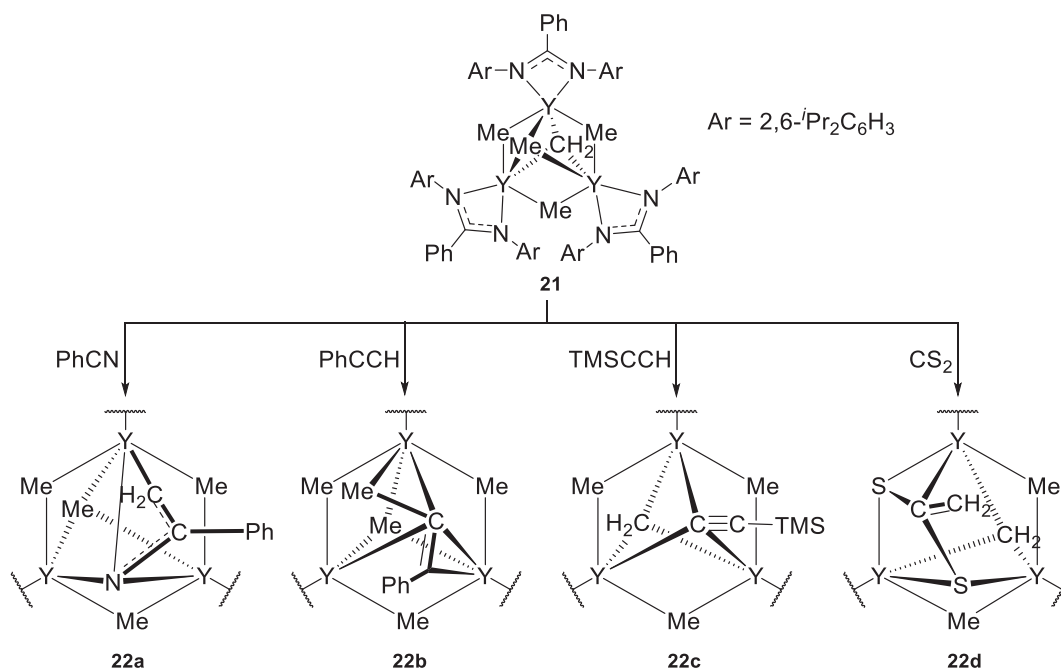
Scheme 16 Regio- and stereoselective isoprene polymerization catalyzed by complex 20/ $[\text{CPh}_3][\text{B}(\text{C}_6\text{F}_5)_4]$.

In subsequent studies, the ^{*t*}Bu substituted amidinate complex $\{((2,6\text{-}i\text{-Pr}_2\text{C}_6\text{H}_3)\text{N})_2\text{C}(\text{}^t\text{Bu})\}\text{Y}(o\text{-CH}_2\text{C}_6\text{H}_4\text{NMe}_2)_2$, (23), and the related dinuclear compound $[(o\text{-CH}_2\text{C}_6\text{H}_4\text{NMe}_2)_2\text{Y}((2,6\text{-}i\text{-Pr}_2\text{C}_6\text{H}_3)\text{N})_2\text{CCH}_2\text{CH}_2\text{CH}_2\text{CH}_2\text{C}(\text{}^t\text{Bu})_2\text{Y}(o\text{-CH}_2\text{C}_6\text{H}_4\text{NMe}_2)_2]$, (24), were established to produce polyisoprene with much narrower molecular weight distributions



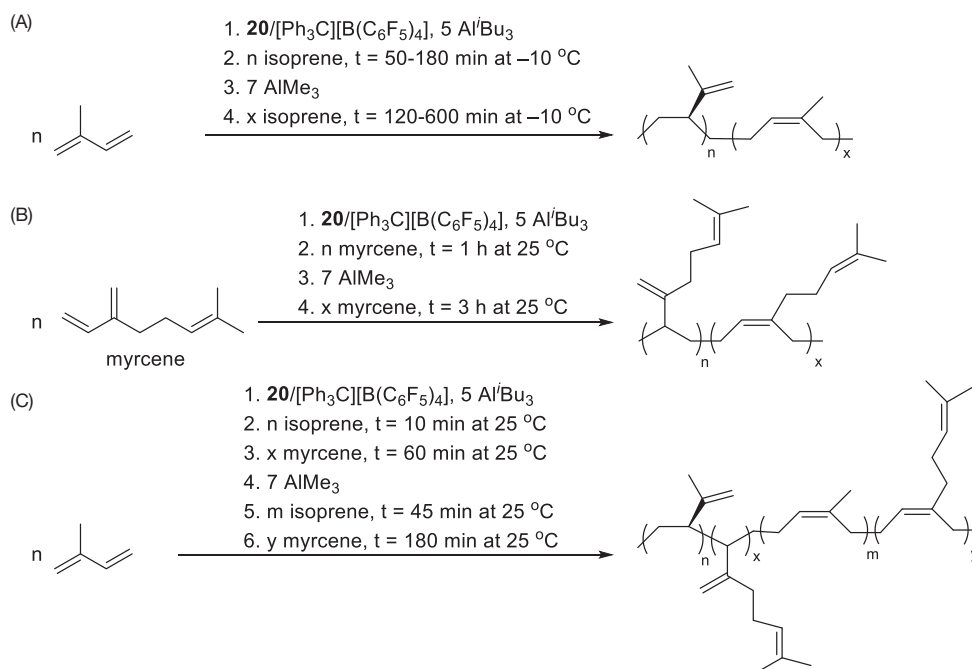
Scheme 17 Reaction of complex (20) with two equivalents of AlMe_3 .

(PDI = 1.10 (23) vs. 1.30 (20)) and higher activity than (20), when activated by only $[\text{Ph}_3\text{C}][\text{B}(\text{C}_6\text{F}_5)_4]$ (Fig. 4).⁴³ The complex (24)/ $[\text{Ph}_3\text{C}][\text{B}(\text{C}_6\text{F}_5)_4]$ system was also used to efficiently synthesize regioregular polymers of isoprene and myrcene at low temper-



Scheme 18 Reaction of complex (21) with terminal nitriles, alkynes and CS₂.

atures (−58 °C) achieving comparable regioselectivity, but with much higher catalyst activity (20: 50 min at −10 °C for 375 equivalents of isoprene, 24: 1.5 min at −58 °C for 1500 equivalents of isoprene).⁴³ However, in this case substantially more AlMe₃ (20 equivalents) was needed to reverse regioselectivity from 3,4- to 1,4-polyisoprene.



Scheme 19 Synthesis of (A) regioregular polyisoprene; (B) regioregular polymyrcene; and (c) regioregular copolymers of polyisoprene and polymyrcene.

Shen and colleagues synthesized the tethered bis(amidinate) ligand $((\text{N}(\text{SiMe}_3)\text{C}(\text{Ph})\text{NCH}_2)_2\text{CH}_2)$ that forms mono- and dinuclear complexes $[\{((\text{SiMe}_3)\text{NC}(\text{Ph})\text{NCH}_2)_2\text{CH}_2\}\text{YCl}]$, (25), $[\text{Y}_2(\mu\text{-}((\text{SiMe}_3)\text{NC}(\text{Ph})\text{NCH}_2)_2\text{CH}_2)_3]$, (26), and $[\text{Li}(\text{DME})_3][\text{Y}\{((\text{SiMe}_3)\text{NC}(\text{Ph})\text{NCH}_2)_2\text{CH}_2\}_3]$, (27), when its lithium salt is reacted with YCl_3 (Scheme 20).⁴⁴ The tethered bis(amidinate) ligands in the dinuclear complex (26) exist exclusively in the bridging mode with the two amidinate functionalities coordinating to separate yttrium centers. The ability of complexes (26) and (27) to catalyze the ring-opening polymerization (ROP) of ϵ -caprolactone (ϵ -CL) was investigated, during which polymer products with unimodal molecular weight distributions were formed. Although binuclear complex (26) was found to be more active (2500 vs. 1100 equivalents of ϵ -CL in 30 min) than the doubly ligated (27), both complexes afforded products with high polydispersity (PDI = 2.22–2.80). The greater activity of complex (27) was attributed to a more accessible metal center, while the high polydispersity of both species may be due to competitive insertion into multiple yttrium–ligand bonds.

Silyl-bridged bis(amidinate) dinuclear yttrium complexes, $[\text{YR}_n\{((2,6\text{-}^i\text{Pr}_2\text{C}_6\text{H}_3)\text{NCPhN})_2\text{SiMe}_2\}]_2$ bearing chloride (28: $\text{R} = \text{Cl}$, $n = 3$), alkyl (29: $\text{R} = \text{CH}_2\text{SiMe}_3$, $n = 2$) and hydride (30: $\text{R} = \text{H}$, $n = 2$) ligands, which were synthesized through a series of salt metathesis and elimination steps, have also been reported by Trifonov et al. (Scheme 21).⁴⁵

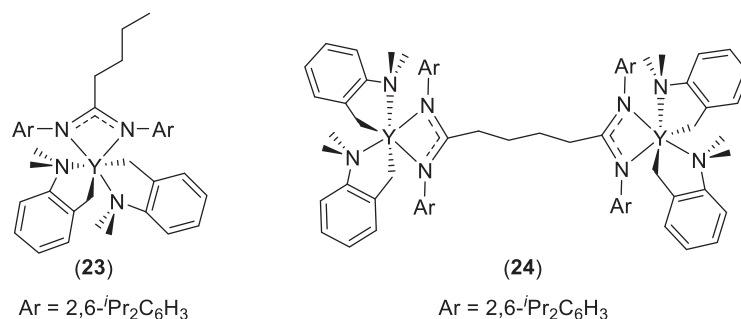
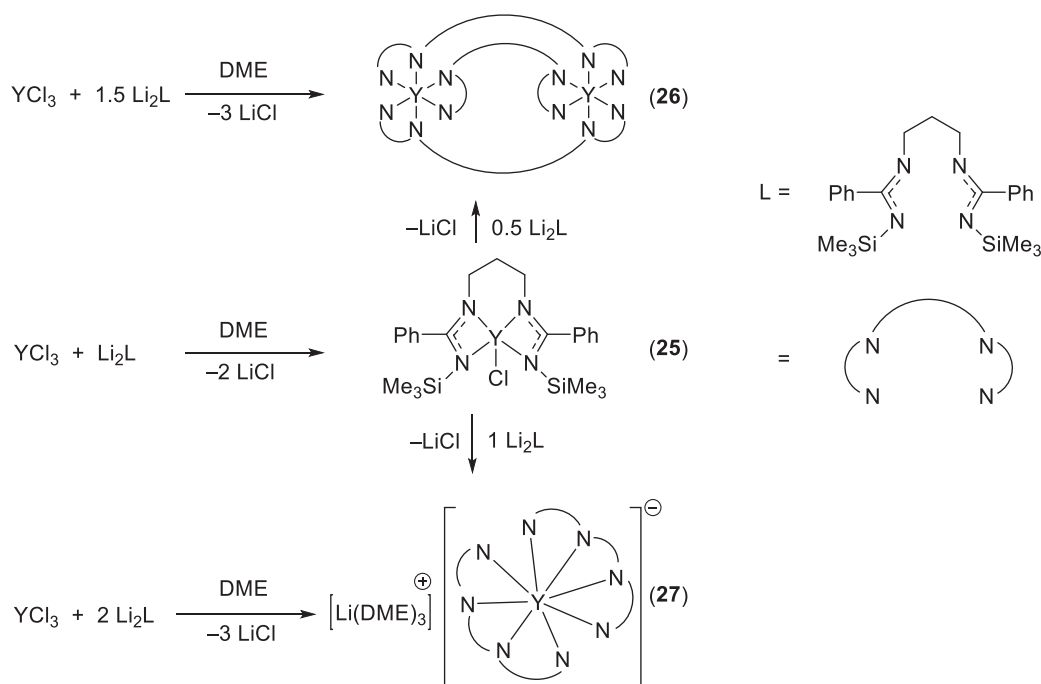


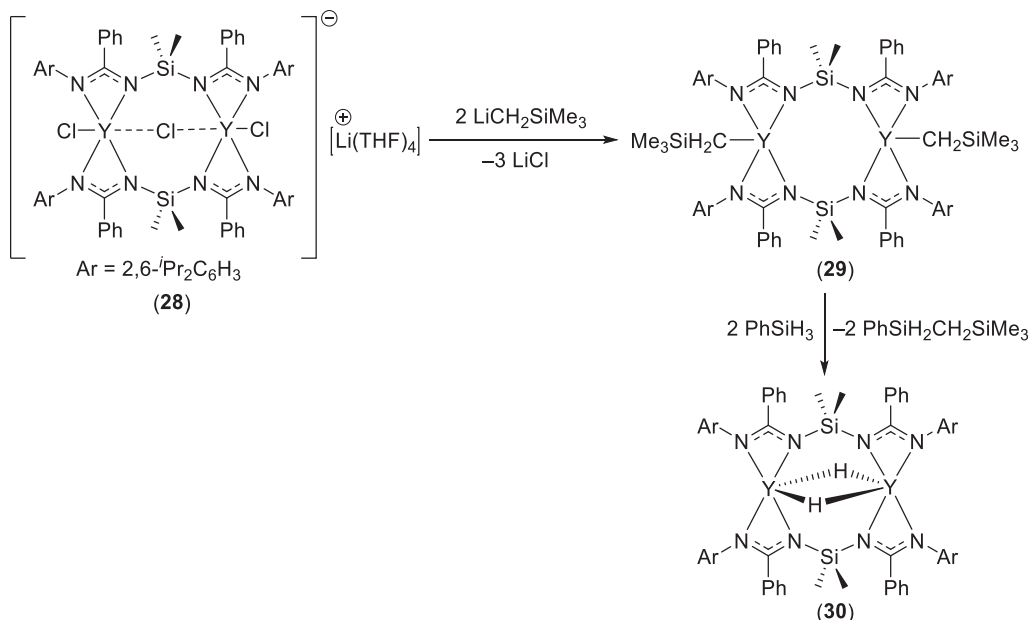
Fig. 4 Monoamidinate complex (23) and tethered bis(amidinate) dinuclear complex (24).

Bis(amidinate) ligands constructed about a phenyl bridge have proven to exhibit several coordination modes that are highly sensitive to the steric bulk of the ligand substituents. Yttrium complexes with 2,6-dimethylphenyl substituents on the ligand backbone featured a κ (4)-bound bis(amidinate), while more sterically demanding 2,6-diisopropylphenyl groups led to tridentate binding modes (Scheme 22A).⁴⁶ While the chloride species $[\{\kappa^4\text{-}1,2\text{-}(\text{NC}(^t\text{Bu})\text{N}(2,6\text{-Me}_2\text{C}_6\text{H}_3))_2\text{C}_6\text{H}_4\}\text{Y}(\mu\text{-Cl})_2\text{Li}(\text{THF})_2]$,



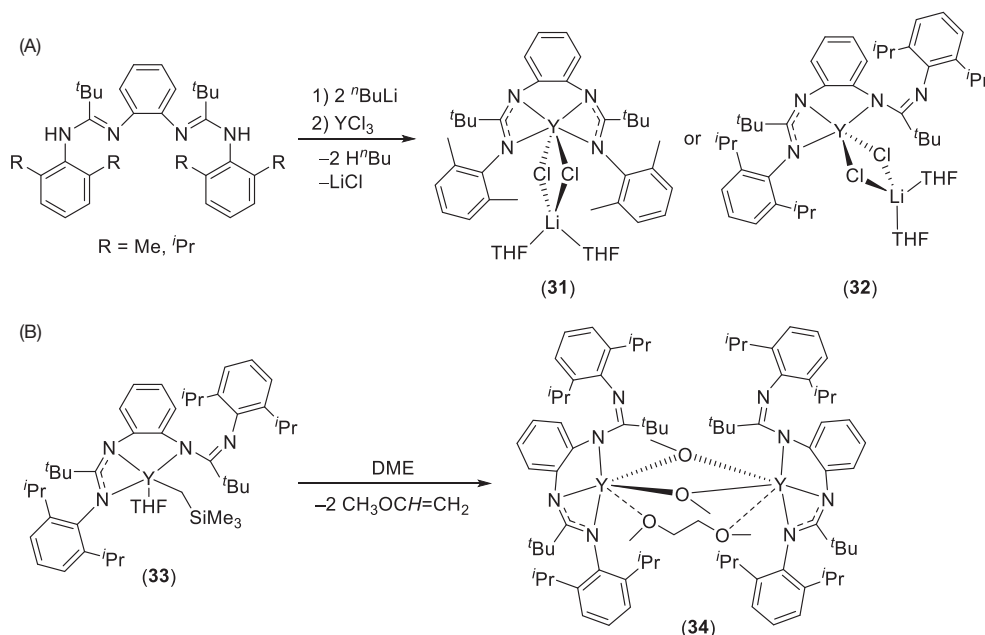
Scheme 20 Synthesis of tethered bis(amidinate) yttrium complexes.

(31), and $[\{\kappa^3\text{-}1,2\text{-}(\text{NC}(\text{tBu})\text{N}(2,6\text{-}i\text{Pr}_2\text{C}_6\text{H}_3))_2\text{C}_6\text{H}_4\}\text{Y}(\mu\text{-Cl})_2\text{Li}(\text{THF})_2]$, (32) did not react with H_2 or PhSiH_3 , the organometallic $[\{\kappa^3\text{-}1,2\text{-}(\text{NC}(\text{tBu})\text{N}(2,6\text{-}i\text{Pr}_2\text{C}_6\text{H}_3))_2\text{C}_6\text{H}_4\}\text{Y}(\text{CH}_2\text{SiMe}_3)(\text{THF})]$, (33), cleaved C–O bonds of DME at ambient temperature to give $[\{\text{Y}\{\kappa^3\text{-}1,2\text{-}(\text{NC}(\text{tBu})\text{N}(2,6\text{-}i\text{Pr}_2\text{C}_6\text{H}_3))_2\text{C}_6\text{H}_4\}_2(\mu\text{-OMe})_2(\mu\text{-MeOCH}_2\text{CH}_2\text{OMe})]$, (34) (Scheme 22B).



Scheme 21 Synthesis of bis(amidinate) stabilized chloride (28), alkyl (29) and hydride (30) complexes.

Analogous complexes bearing borohydride and alkoxide auxiliary ligands (35–38) were studied as potential lactide polymerization catalysts (Fig. 5).^{47,48} All three borohydride species generated atactic polylactide products with moderately narrow molecular weight distributions (PDI = 1.28–2.17). The use of different coordinating solvents had a dramatic effect on the activity of these catalyst systems with the DME ligated complex $[\{1,2\text{-}(\text{NC}(\text{Ph})\text{N}(\text{SiMe}_3))_2\text{C}_6\text{H}_4\}\text{Y}(\text{BH}_4)(\text{DME})]$, (37: 94% conversion of 200 equivalents in 60 min), being more active than the THF coordinated species $[\{1,2\text{-}(\text{NC}(\text{Ph})\text{N}(\text{SiMe}_3))_2\text{C}_6\text{H}_4\}\text{Y}(\text{BH}_4)(\text{THF})_2]$, (36: 40% conversion of 200 equivalents in 60 min).⁴⁷ This difference was largely attributed to the borohydride ligand occupying



Scheme 22 (A) Synthesis of phenyl bridged bis(amidinate) yttrium complexes (31) and (32); and (B) activation of DME by complex (33).

the equatorial position in (36) and the apical site in (37). When tested as hydrophosphonylation catalysts, [$\{1,2\text{-}(\text{NC}(\text{tBu})\text{N}(2,6\text{-Me}_2\text{C}_6\text{H}_3))_2\text{C}_6\text{H}_4\}\text{Y}(\text{BH}_4)(\text{DME})$], (35: 44% conversion in 24 h), exhibited lower activity than complexes (36: 87% conversion in 24 h) and (37: 92% conversion in 24 h) under the same experimental conditions. Alkoxide derivative [$\{1,2\text{-}(\text{NC}(\text{tBu})\text{N}(2,6\text{-Me}_2\text{C}_6\text{H}_3))_2\text{C}_6\text{H}_4\}\text{Y}(\text{O}^t\text{Bu})(\text{DME})$], (38), catalyzed the ring-opening polymerization of 76 equivalents of lactide in toluene over 24 h affording relatively low polydispersity polylactide (PDI = 1.55) (Table 1).⁴⁸

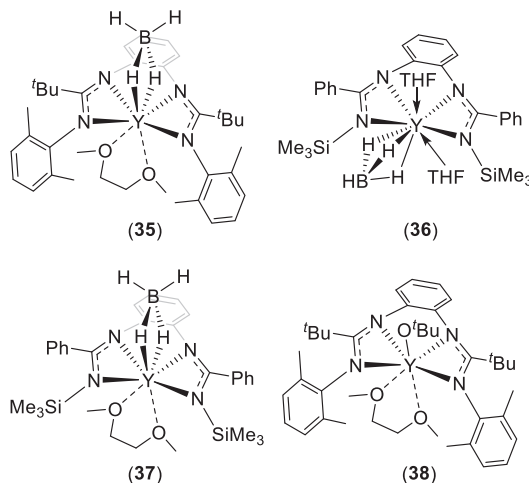


Fig. 5 Phenyl bridged bis(amidinate)-supported borohydride and alkoxide complexes.

Other similar compounds published by the Trifonov group include the naphthalene bridged bis(amidinate) [$\{1,8\text{-}(\text{NC}(\text{tBu})\text{N}(2,6\text{-Me}_2\text{C}_6\text{H}_3))_2\text{C}_{10}\text{H}_6\}\text{Y}(\text{N}(\text{SiMe}_3)_2)$], (39), which is also a competent lactide polymerization (Table 1) and hydrophosphonylation catalyst,⁴⁹ and dialkyl [$\{8\text{-}(\text{NC}(\text{tBu})\text{N}(2,6\text{-}^i\text{Pr}_2\text{C}_6\text{H}_3))\text{NC}_9\text{H}_6\}\text{Y}(\text{CH}_2\text{SiMe}_3)_2$], (40), which is supported by an *N*-functionalized amidinate ligand (Fig. 6; Table 2).⁵⁰

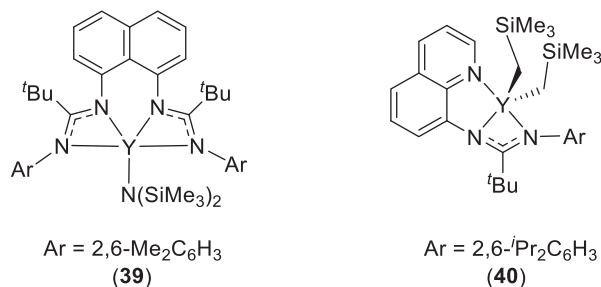


Fig. 6 Naphthalene bridged bis(amidinate) complex (39) and tridentate *N*-functionalized amidinate complex (40).

Table 2 Comparison of catalyst performance for the polymerization of *rac*-Lactide.

Compound	Solvent	Temp (°C)	TOF/h ^{-1a}	M _w /M _n (PDI)	Pr
19a	THF	25	255	1.8	0.78
19b	THF	25	3250	1.72	n.d.
35	Toluene	20	368	1.65	0.56
36	Toluene	20	125	1.45	0.55
37	Toluene	20	355	1.65	0.55
38	Toluene	20	3.17	1.55	n.d.
39	Toluene	25	100	1.37	0.55
48a	THF	20	32.7	1.5	n.d.
48b	Toluene	20	6.64	1.64	n.d.

n.d. = not determined.

^aTOF calculated based on literature provided values.

Chiral amidinate ligands have been used by Roesky to support yttrium complexes $\{[(\text{CH}(\text{Me})(\text{Ph}))\text{N}]_2\text{C}(\text{tBu})\}_2\text{Y}(\text{N}(\text{SiMe}_3)_2)$, (41), and $\{[(\text{CH}(\text{Me})(\text{Ph}))\text{N}]_2\text{C}(\text{tBu})\}_2\text{Y}(\text{CH}(\text{SiMe}_3)_2)$, (42), both of which catalyze the intramolecular hydroamination of aminoalkene/alkyne substrates (Fig. 7).^{51,52} Although these reactions proceed in high yield (>95%) and regioselectivity, poor to moderate enantioselectivity was observed ($ee = 0\text{--}66\%$).

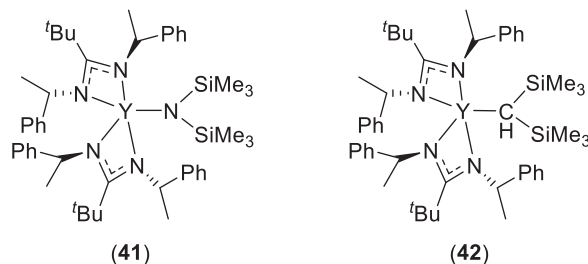
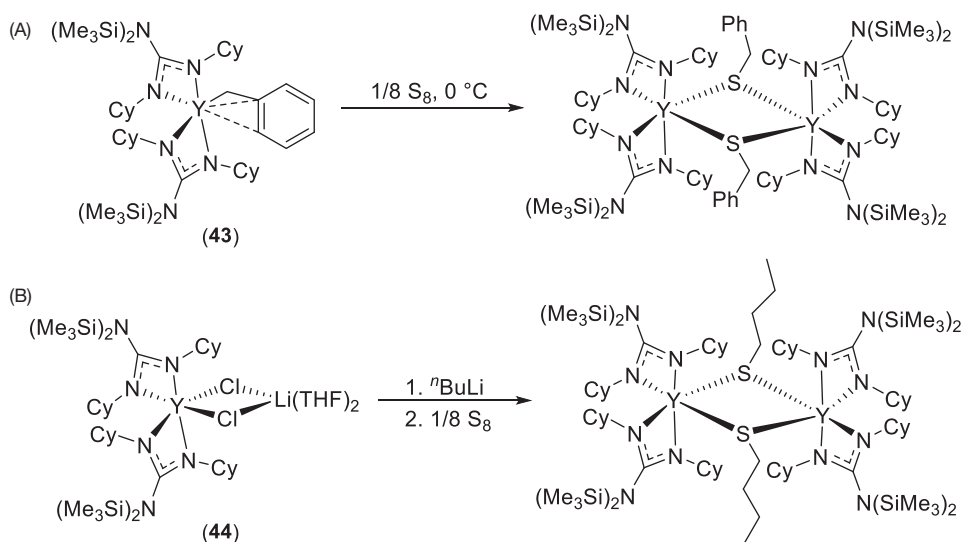


Fig. 7 Chiral amidinate yttrium complexes (41) and (42).

Recent work disclosed by the Zhou group includes the use of bis(guanidinate) aryl complex $\{[(\text{CyN})_2\text{C}(\text{N}(\text{SiMe}_3)_2)]_2\text{Y}(\text{CH}_2(\eta^2\text{-C}_6\text{H}_5))\}$, (43), as an activator for elemental sulfur (Scheme 23A).⁵³ Similarly the bis(guanidinate) "chlor-ate" complex $\{[(\text{CyN})_2\text{-}$



Scheme 23 Activation of elemental sulfur by (A) complex (43); and (B) complex (44).

$\text{C}(\text{N}(\text{SiMe}_3)_2)_2\text{Y}(\mu\text{-Cl}_2)\text{Li}(\text{THF})_2$, (44), reacts sequentially with RLi and S_8 to form analogous disulfide products (Scheme 23B).

Over the past decade the Trifonov group has delved deep into chemical transformations that can be mediated by mono- and bis(guanidinate) yttrium complexes (45–49) (Fig. 8).

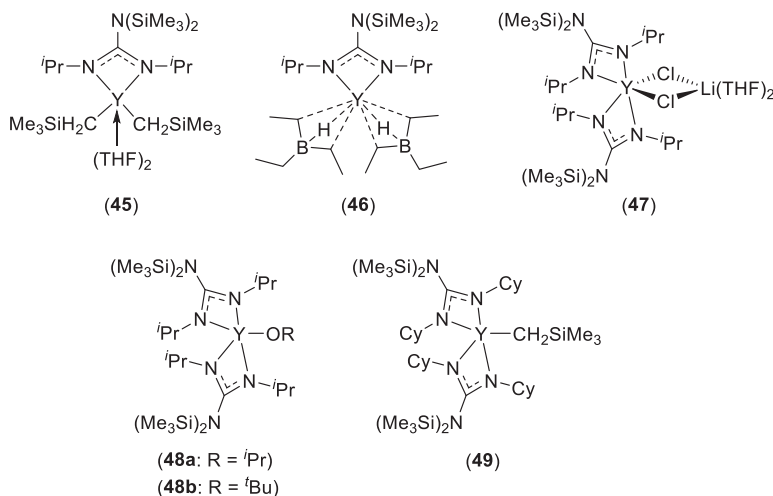
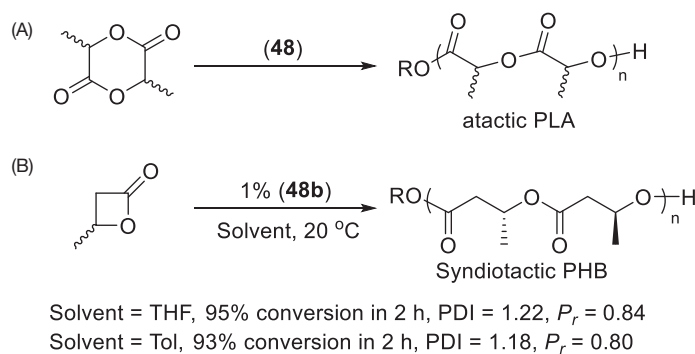


Fig. 8 Guanidinate complexes used by the Trifonov group.

For example, upon addition of 2 equivalents of PhSiH_3 to $[\{(\text{tPrN})_2\text{C}(\text{N}(\text{SiMe}_3)_2)\}\text{Y}(\text{CH}_2\text{SiMe}_3)_2(\text{THF})_2]$, (45), the putative yttrium hydride was generated and established to be marginally active for the polymerization of ethylene (27 equivalents of ethylene were consumed in 3 h at 20 °C in toluene).⁵⁴ Dialkyl (45) also readily reacts with two equivalents of LiBHET_3 to form the bis(borohydride) complex $[\{(\text{tPrN})_2\text{C}(\text{N}(\text{SiMe}_3)_2)\}\text{Y}(\kappa^3\text{-BHET}_3)_2]$, (46).

The related bis(guanidinate) yttrium alkoxides $[\{(\text{tPrN})_2\text{C}(\text{N}(\text{SiMe}_3)_2)\}\text{Y}(\text{O}^i\text{Pr})]$, (48a), and $[\{(\text{tPrN})_2\text{C}(\text{N}(\text{SiMe}_3)_2)\}\text{Y}(\text{O}^i\text{Bu})]$, (48b), were prepared by salt metathesis reactions of the bis(guanidinate) "chloro-ate" complex $[\{(\text{tPrN})_2\text{C}(\text{N}(\text{SiMe}_3)_2)\}\text{Y}(\mu\text{-Cl}_2)\text{Li}(\text{THF})_2]$, (47), and the corresponding alkoxide salt.⁵⁵ While (48a) is stable in both solution and the solid state for several months, the slightly more sterically encumbered (48b) decomposes after prolonged storage. This decomposition is theorized to begin with a 1,3-shift of the SiMe_3 group, followed by C–N bond cleavage in the guanidinate backbone, elimination of $\text{Me}_3\text{SiO}^i\text{Pr}$, and finally, formation of the dinuclear species $[\text{Y}\{(\text{Me}_3\text{Si})_2\text{NC}(\text{N}^i\text{Pr})_2\}_2\{\mu\text{-N}(\text{tPr})\text{C}\equiv\text{N}\}_2]$, along with other unidentified side-products. Both complexes (48a) and (48b) are competent catalysts for the ROP of *rac*-lactide (Scheme 24A and B), and exhibit higher activity in non-coordinating solvents, such as toluene, than in THF. While the polylactide products were found to be atactic, syndiotactic enriched ($P_r = 0.80\text{--}0.84$) polybutyrolactone products were obtained using compound (48b) (Table 1).⁵⁵



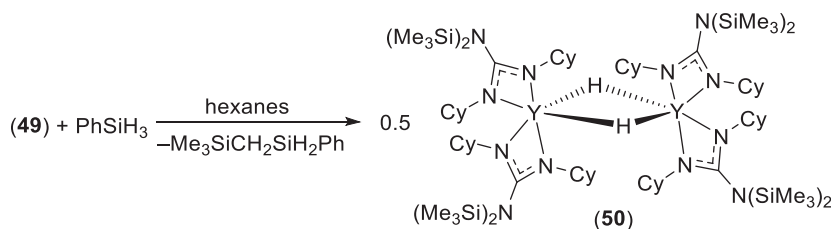
Scheme 24 ROP of (A) *rac*-lactide; and (B) β -butyrolactone catalyzed by complexes (48a,b).

As with its monoguanidinate congener, bis(guanidinate) complex $[\{(\text{CyN})_2\text{C}(\text{N}(\text{SiMe}_3)_2)\}\text{Y}(\text{CH}_2\text{SiMe}_3)]$, (49), reacts with PhSiH_3 to yield a hydride species (Scheme 25).⁵⁶ The well characterized dinuclear hydride, $[\text{Y}\{(\text{CyN})_2\text{C}(\text{N}(\text{SiMe}_3)_2)\}_2(\mu\text{-H})_2]$, (50), is completely inactive toward propylene and styrene and only exhibits low activity for the polymerization of ethylene. However, at a loading of 2% complex (50) quantitatively hydrosilates 1-nonene with PhSiH_3 , giving only the anti-Markovnikov addition product.⁵⁶ Attempts to expand the substrate scope beyond 1-nonene proved unsuccessful.

Nie et al. have synthesized dinuclear $[\text{N}(\text{SiMe}_3)_2\text{Y}\{(\text{tPrN})_2\text{C}(\text{N}_2\text{C}_4\text{H}_8)\text{C}(\text{N}^i\text{Pr})_2\}\text{Y}(\text{N}(\text{SiMe}_3)_2)_2]$, (51), which features an elegant bis(guanidinate) framework wherein the two guanidinate groups are linked by a piperaine moiety.⁵⁷ Complex (51) catalyzes the solvent free hydrophosphonylation of various benzaldehyde and acetophenone derivatives (Scheme 26).

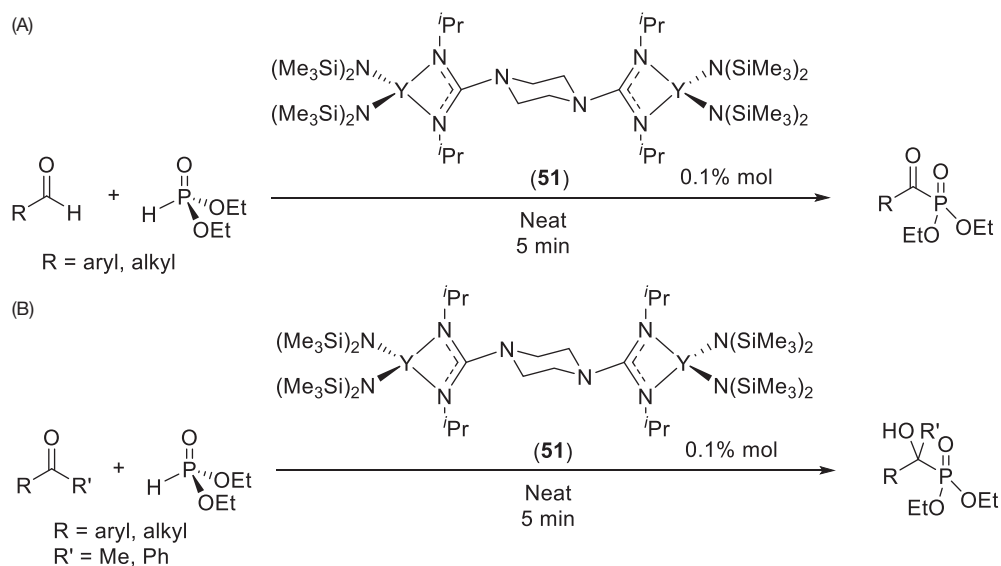
4.03.3.1.3 Iminopyrrolyl ligands

Iminopyrrolyls are an important class of ancillary ligand that feature an imine functionalized pyrrole backbone that can bind to metals *via* an η^2 mode (Fig. 9).⁵⁸ As the imine nitrogen can bear a wide array of substituents, there is additional capacity to fine-tune the steric and electronic properties of the ligand.



Scheme 25 Synthesis of hydride complex (50).

Iminopyrrolyl yttrium complexes are generally prepared according to the previously discussed elimination and salt metathesis protocols, but unlike many other ligands in this article, bis- and even tris(iminopyrrolyl) complexes are commonplace, given the small size of these bidentate frameworks.^{59,60}



Scheme 26 Hydrophosphonylation reactions of (A) benzaldehyde; and (B) acetophenone derivatives catalyzed by piperazine bridged bis(guanidinate) yttrium complex (51).

The Zhou group has reported an unusual method for synthesizing yttrium pyrrolyl complexes wherein the product of the reaction between a pyrrole with a pendant alkylamine is allowed to further react with an yttrium triamido “chlorate” starting material (Scheme 27).⁶¹ This dehydrogenation pathway was investigated and proposed to proceed *via* a β -hydrogen elimination process to yield the bisligated complexes $\{2-(^t\text{BuN}=\text{CH})\text{C}_4\text{H}_2\text{NR}\}_2\text{Y}(\text{N}(\text{SiMe}_3)_2)$, (52a: R = H; 52b: R = ^tBu). While complexes (52) were isolated and characterized, the postulated mechanism leads to many byproducts and has not been fully substantiated.

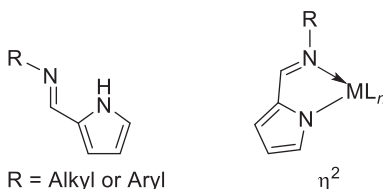


Fig. 9 Generic iminopyrrolyl structure and typical mode of bonding.

Wang et al. utilized tris(iminopyrrolyl) yttrium complexes $[(2-[(2,6-\text{Et}_2\text{C}_6\text{H}_3)\text{N}=\text{CH}](\text{C}_4\text{H}_3\text{N}))_3\text{Y}]$, (53a), and $[(2-[(2,4,6-\text{Me}_3\text{C}_6\text{H}_2)\text{N}=\text{CH}](\text{C}_4\text{H}_3\text{N}))_3\text{Y}(\text{THF})]$, (53b), for ϵ -caprolactone polymerization (Fig. 10).⁵⁹ While both displayed high activities for the catalytic process, the increased steric demand of (53b) yielded polymer products with greater average molecular weights and narrower polydispersities.

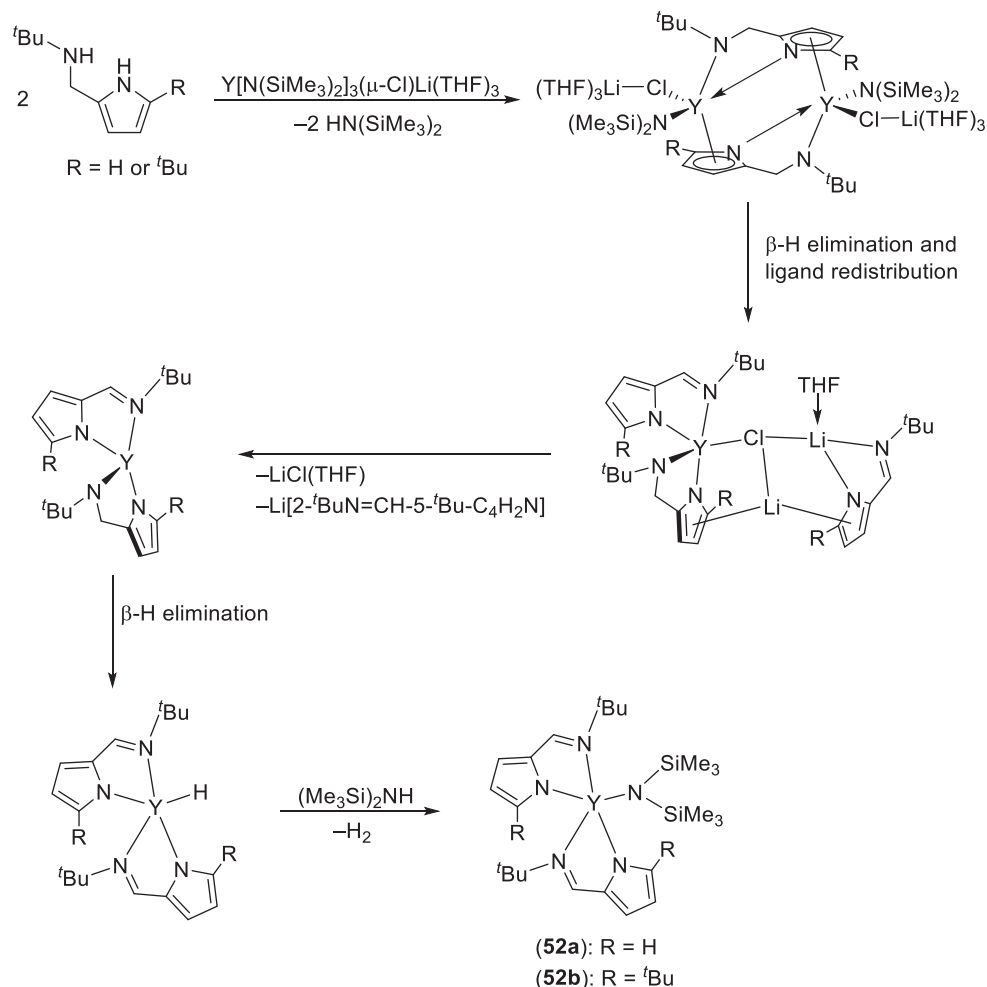
Mashima and co-workers observed backbone methylation when adding bulky iminopyrrolyl ligands to YMe_3 and $\text{Y}(\text{AlMe}_4)_3$ starting materials (Scheme 28A and B).⁶⁰ The resulting aminopyrrolyl bound dimers $[\text{Y}\{2-[(2,6-\text{Me}_2\text{C}_6\text{H}_3)\text{NC}(\text{H})(\text{Me})](\text{C}_5\text{H}_3\text{N})\}\{2-[(2,6-\text{Me}_2\text{C}_6\text{H}_3)\text{N}=\text{CH}](\text{C}_5\text{H}_3\text{N})\}]_2$ (54) and $[\{2-[(2,6-\text{Me}_2\text{C}_6\text{H}_3)\text{NC}(\text{H})(\text{Me})](\text{C}_5\text{H}_3\text{N})\}\text{Y}\{\text{AlMe}_4\}\}]_2$ (55) feature an η^1 nitrogen-bound pyrrole moiety that is coordinated in an η^5 fashion to a second metal center.

A related chiral-bridged bis(iminopyrrolyl) ligand was recently disclosed by Zhou et al.⁶² The corresponding yttrium “ate” complex $[\text{Y}\{(\text{C}_5\text{H}_3\text{N})\text{HC}=\text{N}(\text{PhCHCHPh})\text{N}=\text{CH}(\text{NC}_5\text{H}_3)\}_2(\text{Li}(\text{THF})_2)]$, (56), proved capable of catalyzing the enantioselective epoxidation of α,β -unsaturated ketones (Scheme 29) and although high conversions in THF and toluene were reported, only moderate *ee*'s were observed.

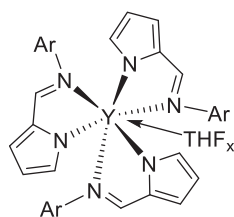
4.03.3.2 Monoanionic, Tridentate N,N,N Donors

4.03.3.2.1 Carbazole and acridanide ligands

Carbazole-based ligands are highly rigid scaffolds capable of providing well-defined coordination environments. As substitution preferentially occurs at the 3 and 6 positions, these sites are typically blocked with Me or ^tBu groups which can be installed *via* Friedel-Crafts⁶³ or bromination methodologies (Fig. 11).⁶⁴ Subsequent derivation at the 1 and 8 sites can afford tridentate ligands capable of stabilizing rare earth elements.^{12,16} Rare earth and transition metal complexes stabilized by pincer ligands with



Scheme 27 Proposed mechanism for the formation of iminopyrrolyl substituted yttrium complexes starting from aminopyrrole and tris(amide) yttrium “chlor-ate” starting materials.



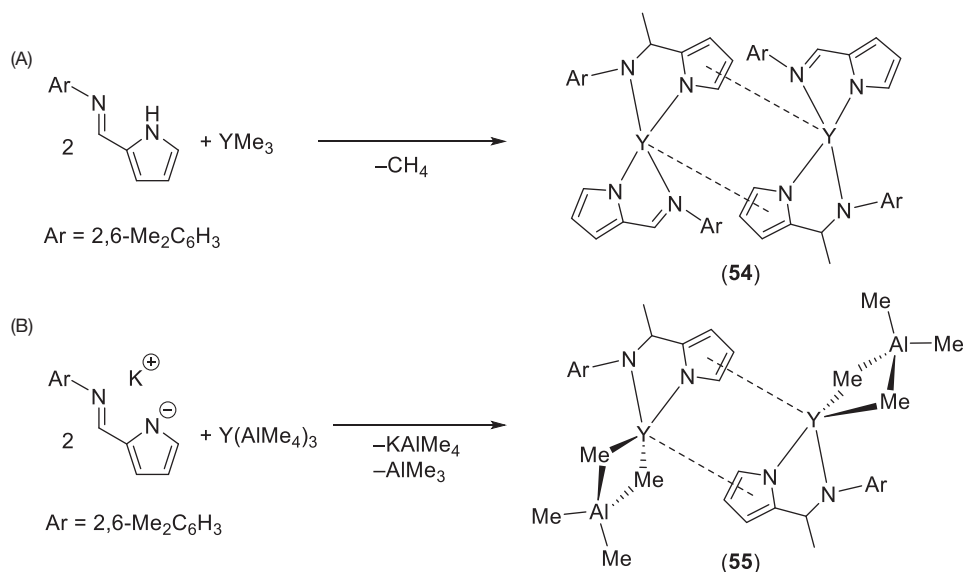
(53a): $\text{Ar} = 2,6\text{-Et}_2\text{C}_6\text{H}_3$, $x = 0$
(53b): $\text{Ar} = 2,4,6\text{-Me}_3\text{C}_6\text{H}_2$, $x = 1$

Fig. 10 Complexes **(53a)** and **(53b)** used by the Wang group for ϵ -caprolactone polymerization.

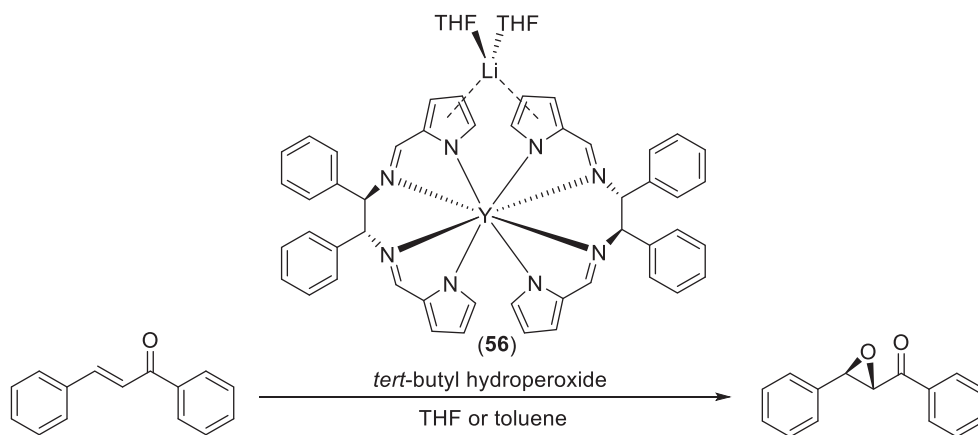
a carbazole core have demonstrated high activity as asymmetric catalysts for a number of reactions, including the polymerization of conjugated dienes and Nozaki-Hiyama coupling, prompting recent studies on such species.^{65–68}

Acridanide-based ligands are similar in structure to their carbazole brethren, but contain an additional carbon atom in the central heterocycle that can be readily functionalized.⁶⁹

Berg et al. utilized bisoxazoline substituted carbazole ligands to form highly stable dichloride [$\{1,8\text{-(4,4'\text{-Me}_2\text{C}_3\text{H}_2\text{NO})\text{-}3,6\text{-tBu}_2\text{-carbazole}\}\text{YCl}_2(\text{THF})\}$], **(57)**, and dialkyl yttrium [$\{1,8\text{-(4,4'\text{-Me}_2\text{C}_3\text{H}_2\text{NO})\text{-}3,6\text{-tBu}_2\text{-carbazole}\}\text{Y}(\text{CH}_2\text{SiMe}_3)_2$], **(58)**, complexes (**Scheme 30**).⁶³



Scheme 28 Formation of methylated aminopyrrolyl complexes (54) and (55) from (A) YMe_3 ; and (B) $Y(AlMe_4)_3$.



Scheme 29 Enantioselective epoxidation of α,β -unsaturated ketones catalyzed by complex (56).

Due to the bulky nature of oxazoline groups, the two CH_2SiMe_3 substituents in (58) bend toward the plane of the carbazole backbone, providing a “folded wing” structure (*vide supra*). This geometry is suspected to hinder alkene coordination; complex (58) does not polymerize ethylene, isoprene or 2,3-dimethylbutadiene, even upon addition of $[Ph_3C][B(C_6F_5)_4]$ as an activator.

A related carbazole system that features two phosphinimine donors was published by Hayes et al. in 2014. In this case mesitylene (Mes) groups were added to saturate the metal's coordination sphere,⁷⁰ and although the resultant yttrium dichloride species $\{1,8-[(2,4,6-Me_3C_6H_2)N=PPh_2]_{2-3,6-Me_2-carbazole}\}YCl_2$, (59), was found to be both monomeric and THF-free, the corresponding organoyttrium complex $\{1,8-[(2,4,6-Me_3C_6H_2)N=PPh_2]_{2-3,6-Me_2-carbazole}\}Y(CH_2SiMe_3)_2$, (60), succumbed to rapid decomposition by double P–Ph cyclometalation to afford $[Y\{\kappa^3N,\kappa^2C:1,8-[(2,4,6-Me_3C_6H_2)N=PPh(C_6H_4)]_{2-3,6-Me_2-carbazole}\}]$, (61) (Scheme 31).

Emslie and co-workers have synthesized a diphenylmethylenamido derived acridanide ligand that was also prone to decomposition *via* cyclometalation when coordinated to yttrium.⁶⁹ Upon reaction of their ligand ($L = [4,5-(N=C(Ph)_2)-2,7,9,9-Me_4-acridanide]$) with $Y(CH_2SiMe_3)(THF)_2$, neither X-ray crystallography nor NMR data revealed evidence for the formation of

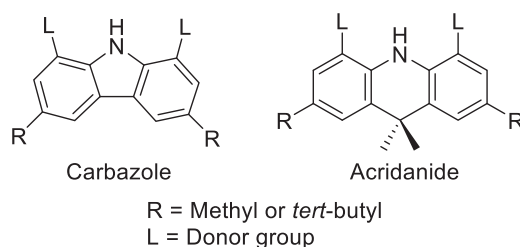
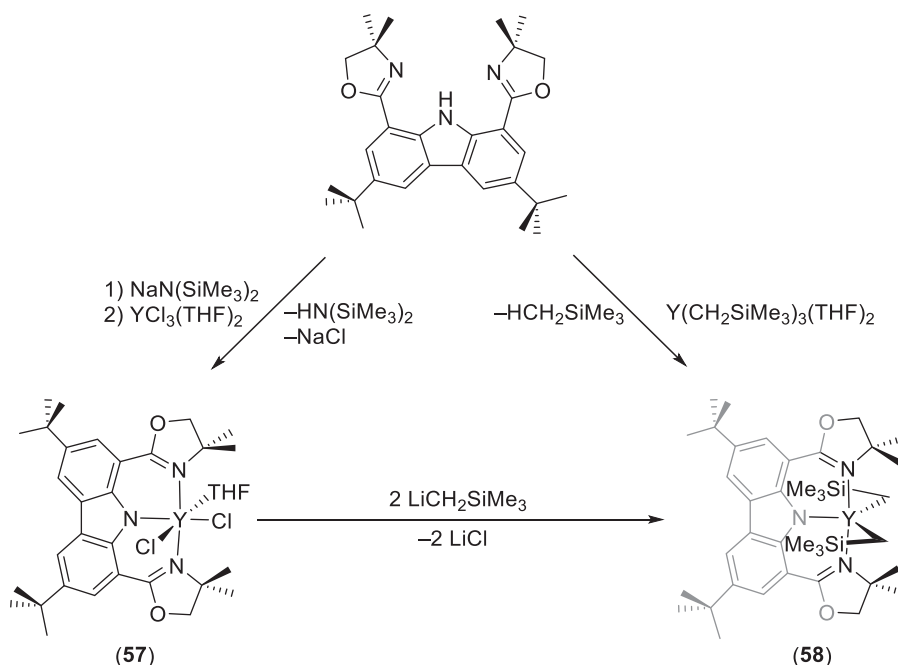


Fig. 11 Generic structures of carbazole and acridanide ancillary ligands.

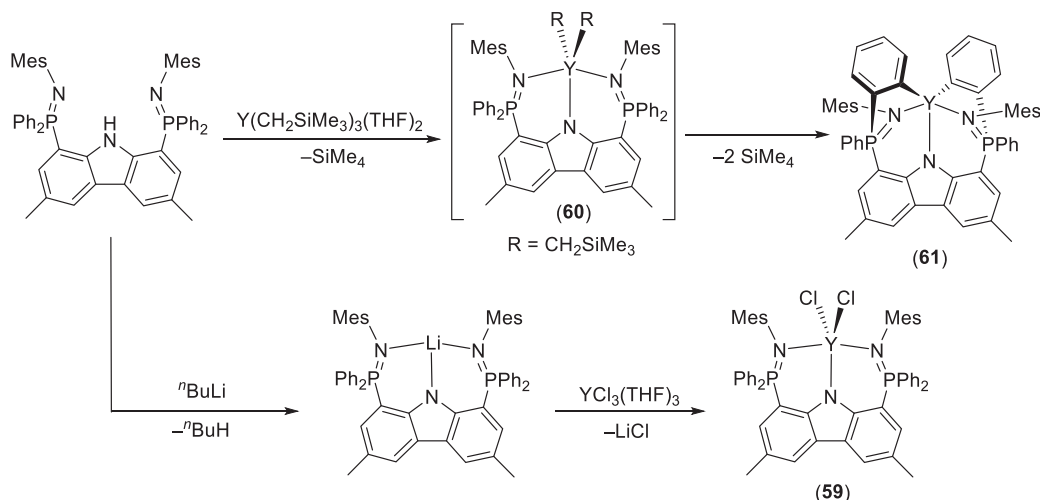
[LY(CH₂SiMe₃)₂] or [L₂Y(CH₂SiMe₃)]*—*only the cyclometalated bisligated complex [Y{κ³N:4,5-(N=C(Ph)₂)-2,7,9,9-Me₄-acridanide}{κ⁴N,N,N,C:4-(N=C(Ph)₂)-5-(N=C(Ph)(C₆H₄))-2,7,9,9-Me₄-acridanide}], (62), was observed. Complex (62) contains one unadulterated ligand, and one that is cyclometalated at the *ortho* position of a phenyl group. When left in solution over 3 days, complex (62) underwent further rearrangement to ultimately afford complex (63), presumably *via* two sequential 1,2 insertion processes (Scheme 32).



Scheme 30 Bisoxazoline substituted carbazole pincer ligand and yttrium complexes thereof.

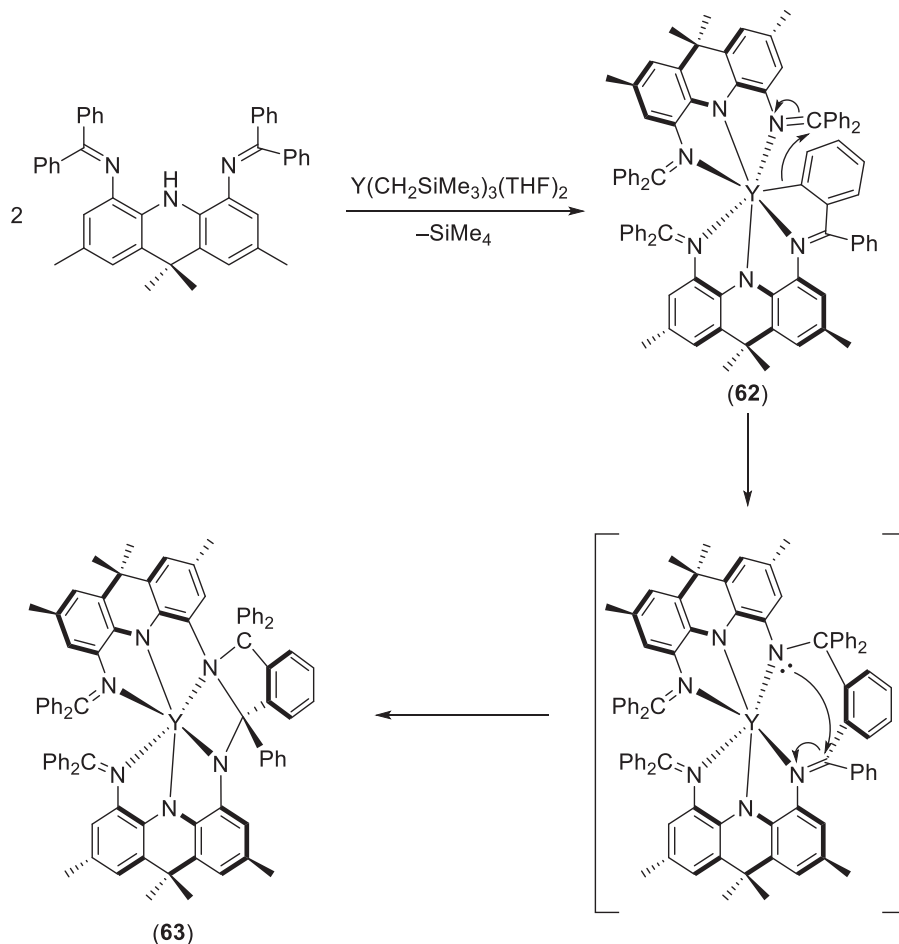
4.03.3.2.2 Tris(Pyrazolyl)borate scaffolds

Trispyrazole scorpionate frameworks, such as tris(pyrazolyl)borate (Tp^{R,R'}, R,R' = Me, ^{*i*}Pr, ^{*t*}Bu, H), are a class of highly versatile ligand that is widely exploited in inorganic chemistry (Fig. 12).^{71,72} Steric bulk can be readily fine-tuned by incorporating substituents on the 3 and 5 positions of the pyrazolyl rings, which can also impact the bite and cone angles of the ligand. These factors make Tp^{R,R'} ligands highly appealing for use in yttrium chemistry wherein the ability to easily adjust the coordination environment is highly desirable in the quest for thermally robust complexes.



Scheme 31 Synthesis of yttrium complexes (59–61) supported by a monoanionic *MWN*-bisphosphinimine carbazole architecture.

Synthesis of yttrium tris(pyrazolyl) borate complexes follows typical salt metathesis and alkane elimination pathways (Scheme 33A–C). Alkane elimination requires the acid form of the $\text{Tp}^{\text{R,R'}}$ ligands, the availability and stability of which are heavily dependent on the steric bulk of R and R'.¹⁶ Takats et al. have demonstrated the viability of using $\text{Ti}(\text{Tp}^{\text{R,R'}})$ starting materials as alkyl abstraction agents to transfer smaller and less stable Tp^{Me_2} ligands to yttrium (Scheme 33C).^{74,75}



Scheme 32 Formation and subsequent rearrangement of complex (62) to (63).

As a testament to the high stability offered by Tp ligands, the same group was able to synthesize a family of yttrium dihydride complexes, $[\text{Tp}^{\text{R}_2}\text{YH}_2(\text{THF})_x]_n$ (64a: R = Me, $n = 4$, $x = 0$ in toluene or Et_2O , $n = 3$, $x = 1$ in THF; 64b: R = H, $n = 6$, $x = 0$; 64c: R = $t\text{Pr}$, $n = 3$, $x = 0$) which are amongst the few examples of non-cyclopentadienyl rare earth dihydride compounds (Scheme 34).⁷⁴ These dihydride complexes exist in complicated asymmetric cluster formations that vary depending upon solvent. When Tp^{Me_2} was utilized, a tetranuclear cluster was isolated when the hydrogenolysis was conducted in toluene or diethylether, but a tri-

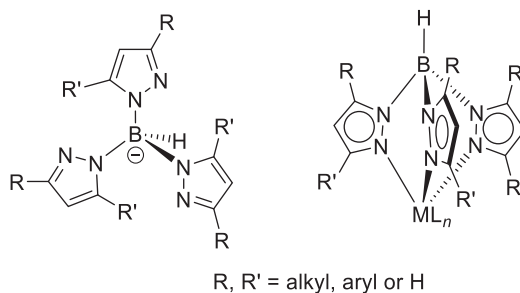
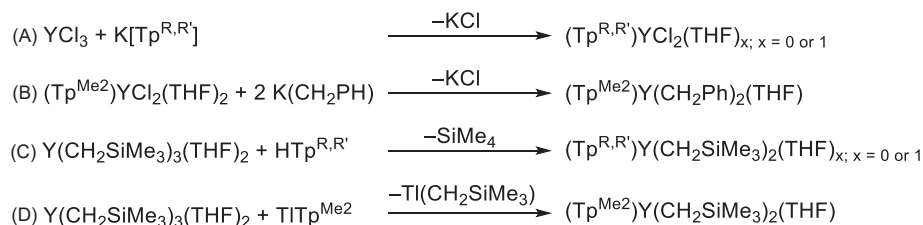


Fig. 12 Generic structure and bonding motif of tris(pyrazolyl)borate ligands.

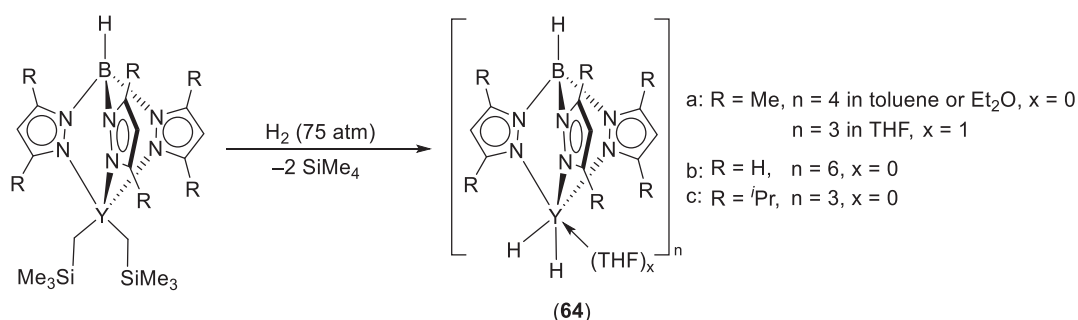
nuclear THF adduct was obtained when the reaction was performed in THF.^{75,76} When the unsubstituted Tp ligand was utilized, a mixture of products prevailed, from which a hexanuclear cluster was established to be the predominant product. Conversely,

the larger $\text{Tp}^{\text{Pr}2}$ variant afforded a trinuclear compound *sans* solvent coordination. In all cases the hydrides exhibited a variety of bridging bonding modes (μ_2 , μ_3 , μ_4) between yttrium centers.



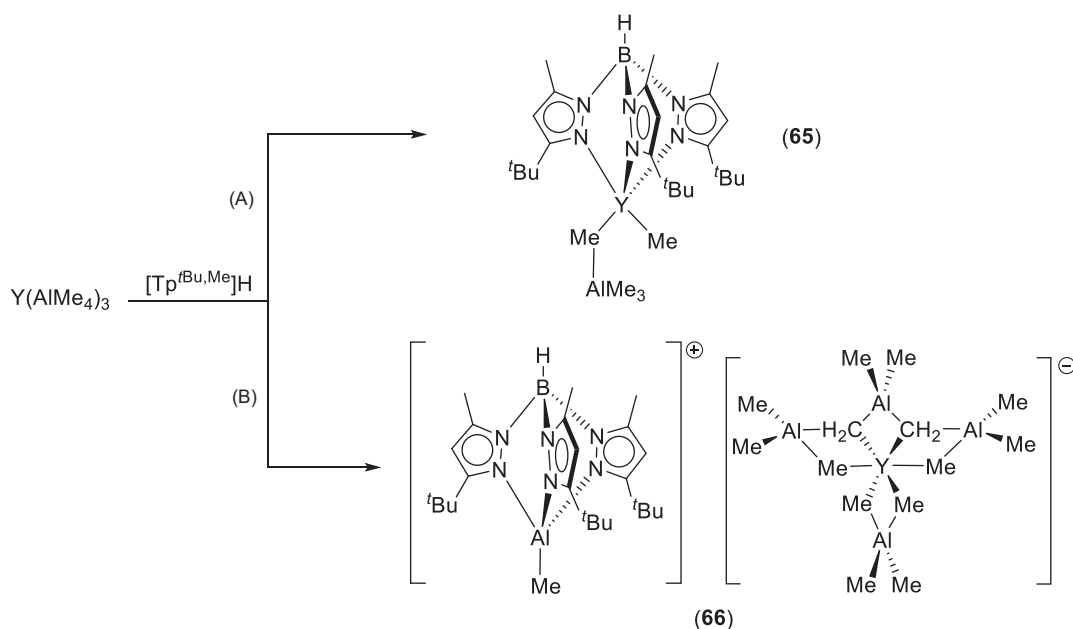
Scheme 33 General synthetic routes to $\text{Tp}^{\text{R,R}'}$ yttrium complexes: (A and B) Salt metathesis and subsequent derivatization⁷³; (C) alkane elimination; (D) thallium transfer agents.

The Anwander group has explored the chemistry of $[\text{Tp}^{\text{tBu,Me}}]\text{H}$ and $\text{Y}(\text{AlMe}_4)_3$ (Scheme 35A),^{77,78} which led to $[(\text{Tp}^{\text{tBu,Me}})\text{Y}(\text{AlMe}_4)(\text{Me})]$, (65), a complex that features rapidly exchanging AlMe_4 and Me ligands on the ^1H NMR timescale. The byproduct $[\text{Tp}^{\text{tBu,Me}}\text{AlMe}][\text{Y}(\text{AlMe}_4)(\text{Al}_3\text{Me}_3(\text{CH}_2)_2)]$, (66), resulted from the addition of $[\text{Tp}^{\text{tBu,Me}}]^-$ to AlMe_4 , which ultimately led to the formation of an yttrium methylaluminum cluster that exists as an ionic pair (Scheme 35B).



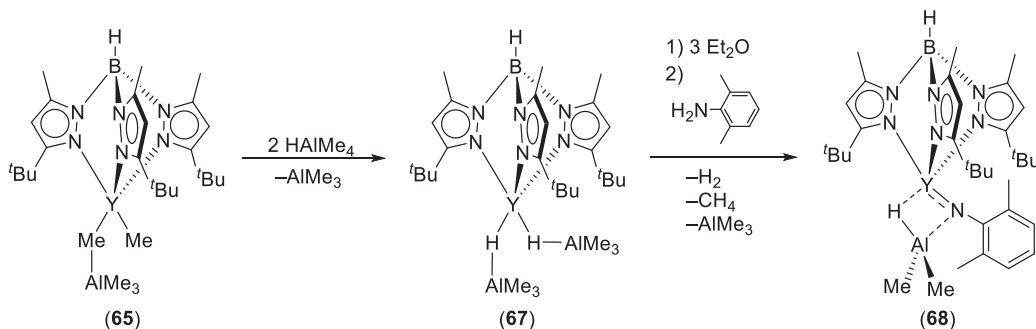
Scheme 34 Synthesis of Tp-supported dihydride yttrium clusters.

Addition of 2 equivalents of HALMe_2 to complex (65) formed the trimethylaluminum terminated dihydride $[(\text{Tp}^{\text{tBu,Me}})\text{Y}((\mu\text{-H})\text{AlMe}_2)_2]$, (67), which displays hydride-like reactivity upon exposure to 2,6-dimethylaniline to form an imide complex in an arrested state of hydroalumination, $[(\text{Tp}^{\text{tBu,Me}})\text{Y}\{(\mu\text{-H})-(\mu\text{-N}(2,6\text{-Me}_2\text{C}_6\text{H}_3))\text{AlMe}_2\}]$, (68) (Scheme 36).⁷⁹



Scheme 35 Addition of $[\text{Tp}^{\text{tBu,Me}}]\text{H}$ to $\text{Y}(\text{AlMe}_4)_3$ to form (A) complex (65); and (B) byproduct (66).

Notably, when the gallium analogue of complex (65) was treated with 2,6-dimethylaniline, the mixed alkylamido complex [(Tp^{tBu,Me})Y(NH(2,6-Me₂C₆H₃))Me], (69), was generated. Subsequent addition of 4-dimethylaminopyridine (DMAP) to complex (69), afforded one of the first terminal imido complexes of a rare earth metal, [(Tp^{tBu,Me})Y=N(2,6-Me₂C₆H₃)](DMAP)], (70) (Scheme 37).⁸⁰ Notable, the authors have not reported whether similar chemistry takes place with complex (65).

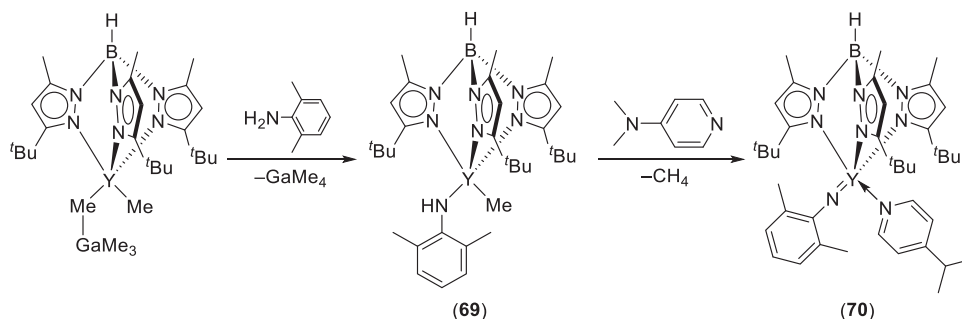


Scheme 36 Formation of trimethylaluminum terminated dihydride complex (67) and imido complex (68).

An array of mixed Cp/Tp^{Me₂} yttrium alkyl, phosphide and acetylide species have also been reported (Fig. 13).^{73,81–86} The reactivity of these species with unsaturated organic compounds was described in a series of papers by Zhang et al.

Specifically, complexes [(Tp^{Me₂})Y(Cp)(CH₂Ph)(THF)], (71), and [(Tp^{Me₂})Y(Cp)(C≡CPh)(THF)], (72), reacted readily with carbodiimides, isocyanates, isothiocyanates and CS₂ to afford the corresponding insertion products (Scheme 38A and B).⁸¹ Notably, [(Tp^{Me₂})Y(Cp)(PPh₂)(THF)], (73), is an active catalyst for the cross-coupling of phenylacetylene and carbodiimides.⁸³

In addition, complex (71) exhibits high activity toward organonitriles, forming unique insertion and cyclization products when multiple equivalents are added at elevated temperatures (Scheme 39).⁸²



Scheme 37 Synthesis of a terminal yttrium imide.

Complex (73) reacts with phenyl isocyanate and phenyl isothiocyanate by insertion into the Y–P σ-bond, to yield [(Tp^{Me₂})Y(Cp)(κ²-N,O:(Ph)NC(PPh₂O)(THF)], (74), and [(Tp^{Me₂})Y(Cp)((κ²-N,S:(Ph)NC(PPh₂S)(THF)], (75), respectively (Scheme 40).⁸³ When multiple equivalents of phenyl isocyanate were added to complex (74) the double insertion, as well as catalytic cyclo-trimerization (10% catalyst loading at ambient temperature in THF gave 83% conversion) products were observed.⁸³

The Zhang group have also explored non-Cp analogues of yttrium Tp systems. When potassium guanidinate K[(^tPrN)₂CN(-SiMe₃)₂] was allowed to react with the dichloride complex [(Tp^{Me₂})YCl₂(THF)], (76), the mixed chloride/amide complex

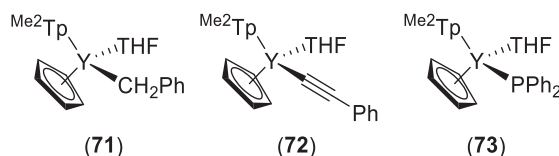
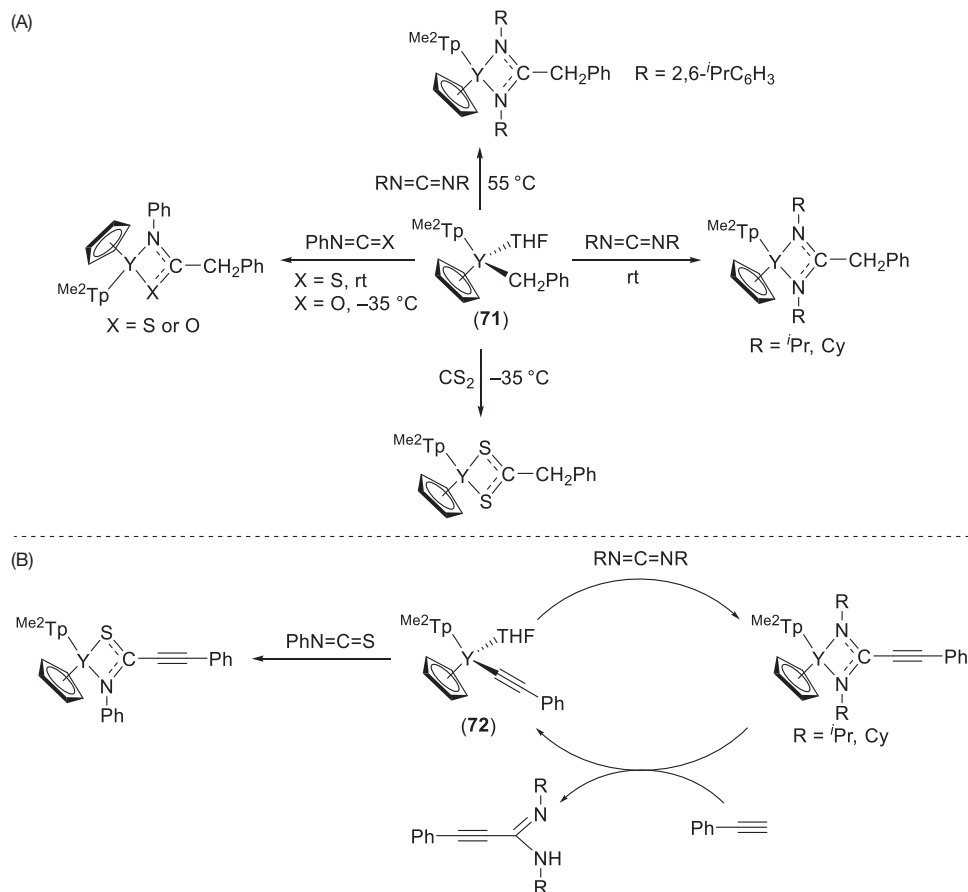


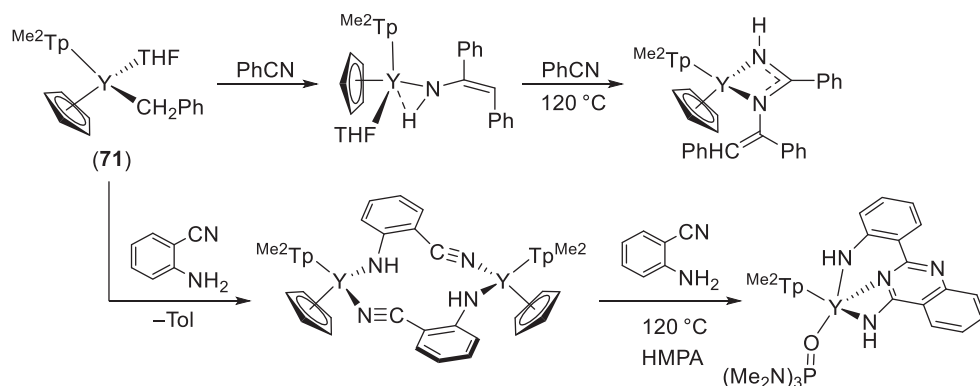
Fig. 13 Mixed Cp/Tp^{Me₂} yttrium complexes.

[(Tp^{Me₂})Y(N(SiMe₃)₂)Cl(THF)], (77), was generated *via* an unusual deinsertion of the carbodiimide moiety.⁸⁴ Complex (77) appears to undergo Si–Me cleavage when a second equivalent of potassium guanidinate is added, forming [(Tp^{Me₂})Y{(^tPrN)₂CN(-Me)}(N(SiMe₃)₂)], (78a) and 0.5 equivalents of the cyclic byproduct [(Me₃Si)N(μ₂-SiMe₂)₂], (78b) (Scheme 41).



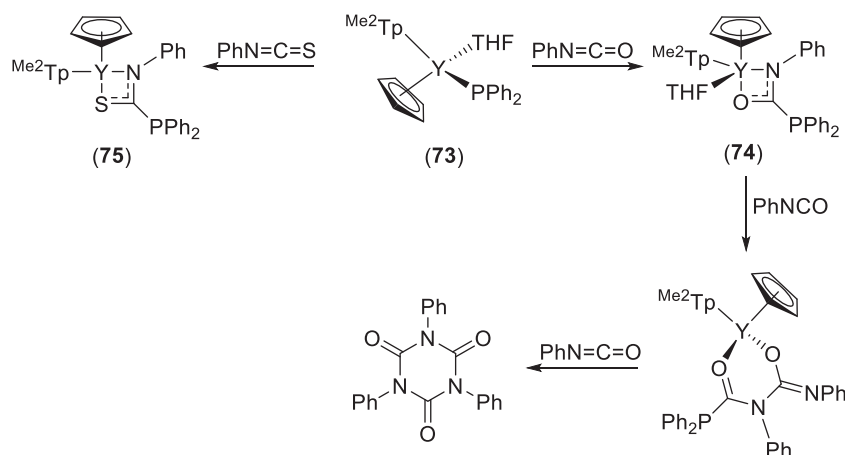
Scheme 38 Reaction chemistry of complexes (A) (**71**); and (B) (**72**) with carbodiimines, phenylisocyanate, phenylisothiocyanate and CS₂.

The related dibenzyl Tp^{Me2} complex [(Tp^{Me2})Y(CH₂Ph)₂(THF)], (**79**), also exhibited rich reaction chemistry with amines and unsaturated organic molecules. For example, reaction of (**79**) with aryl amines formed the primary amido complexes [(Tp^{Me2})Y(CH₂Ph)(NHAr)(THF)], (**80a**: Ar = 2,6-*i*-Pr₂C₆H₃; **80b**: Ar = Ph), that undergo selective insertions that appear to be dictated by the steric bulk of the carbodiimide (**Scheme 42**, left).⁸⁵ Reactions with phenyl isocyanate, phenyl isothiocyanate and phenyl aceto-



Scheme 39 Reaction of complex (**71**) with organonitriles

nitrile provided [(Tp^{Me2})Y(THF){μ-η¹:η³-OC(CHPh)NPh}{μ-η³:η²-OC-(CHPh)NPh}Y(Tp^{Me2})], (**81**), [(Tp^{Me2})Y(μ₃-S)]₄, (**82**), and [{(Tp^{Me2})Y}₂(μ-3,5-Me₂N₂C₃H)₂{μ-η¹:η³-NC(CH₂Ph)CHPh}], (**83**), respectively (**Scheme 42**, right).⁷³ Reactions with *N*-heterocycles resulted in unexpected reactivity depending on the substrate used.⁸⁶ When (**79**) was added to 2 equivalents of

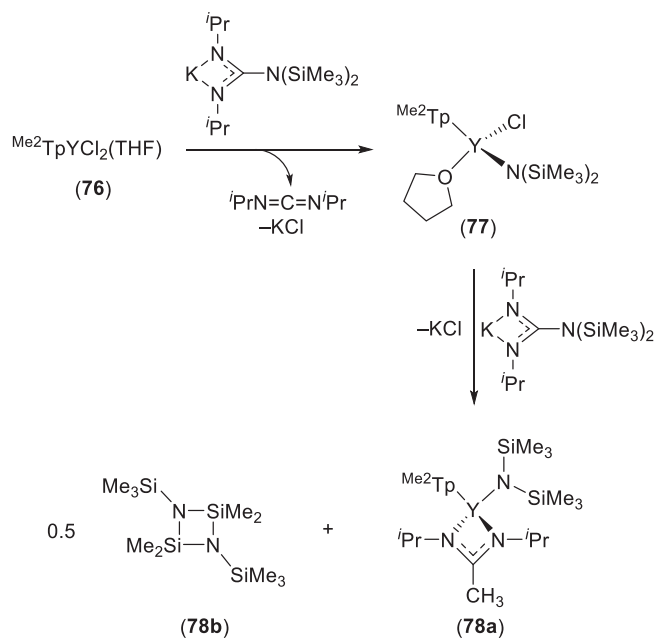


Scheme 40 Reaction of complex (73) with phenyl isocyanate and phenyl isothiocyanate.

1-methylimidazole, a hexanuclear 24-membered metallocyclic compound was afforded through C–H activations at the C2- and C5-positions of the imidazole ring. Reactions with other substrates, such as 1-methylbenzimidazole and benzothiazole, resulted in C–C coupling and ring-opening events.

4.03.3.2.3 NNN-Pyrrole-based ligands

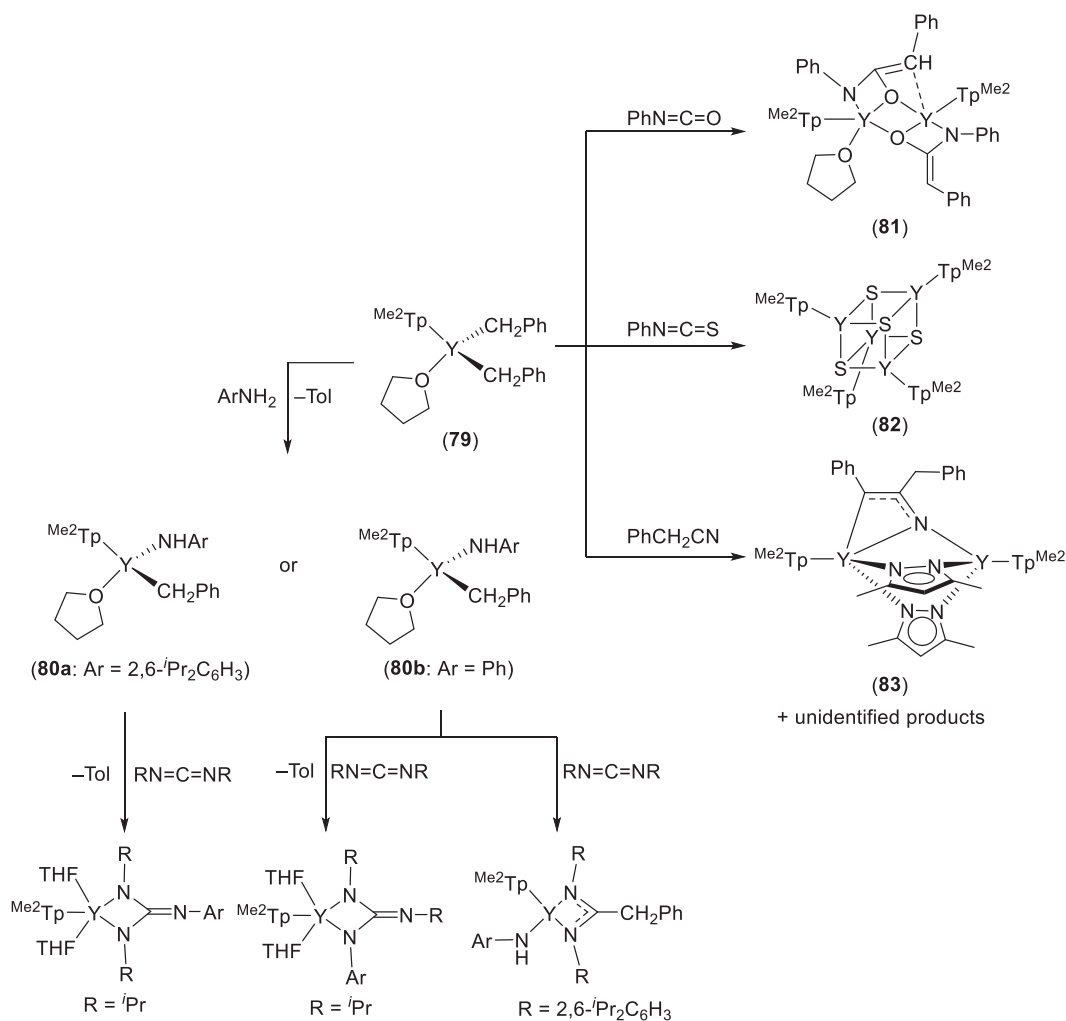
Disubstituted pyrrole-based ligands generally chelate to metal centers to form two five membered rings (Fig. 14). Such ligand sets feature a rigid core that is flanked by flexible, electron-rich donors, such as amines, imines or phosphinimines. Derivatization of the



Scheme 41 Sequential reaction of complex (77) with one and two equivalents of potassium guanidinate.

donor “arms” is facile, with aryl and cyclic alkyl groups commonly incorporated. As a consequence of their steric and electronic versatility, these monoanionic ligands have found utility supporting monometallic dialkyl yttrium complexes.

In 2008, Roesky and co-workers prepared [$\{2,5-(C_4H_8NCH_2)_2C_4H_2N\}Y(CH_2SiMe_3)_2$], (84), by a standard alkane elimination reaction between the proteo ligand ($L = (2,5-(C_xH_yNCH_2)_2C_4H_2NH)$, $x = 4$, $y = 8$ or $x = 5$, $y = 10$) and $Y(CH_2SiMe_3)_2$. Intriguingly, when the pendant amine donor ring size increased from 5 (pyrrolidine) to 6 (piperidine) the putative dialkyl product [$\{2,5-(C_5H_{10}NCH_2)_2C_4H_2N\}Y(CH_2SiMe_3)_2$], (85a), was not observed. Instead, dinuclear [$\{\mu-\eta^5:\eta^5:\eta^1:\eta^1:2,5-(C_5H_{10}NCH_2)_2C_4H_2N\}_2(Y(CH_2SiMe_3)_2)_2$], (85b), which features both η^5 and η^1 Y-pyrrole bonding, was the exclusive product (Scheme 43).⁸⁷ Upon in situ activation with $[Ph_3C][B(C_6F_5)_4]$ both complexes (84) and (85b) exhibited moderate catalytic activity



Scheme 42 Reaction of complex **79** with (left) aryl amines followed by carbodiimides; and (right) phenyl isocyanate, phenyl isothiocyanate, and phenyl acetonitrile.

for isoprene polymerization, generating polymers with high *cis*-1,4 selectivity (80–94%) and narrow molecular weight distributions ($M_w/M_n = 1.05$ –1.22).

As illustrated by Roesky, Hayes and colleagues discovered that small changes in ligand architecture can have a profound impact on the stability of organometallic yttrium complexes. Specifically, the bisphosphinimine pyrrole complex [$\{2,5-(p\text{-}i\text{PrC}_6\text{H}_4)\text{N}=\text{P}(\text{Ph})_2\text{C}_5\text{H}_2\text{N}\}\text{Y}(\text{CH}_2\text{SiMe}_3)_2$], (**86**), proved to be thermally stable in benzene-*d*₆ solution for an extended period at

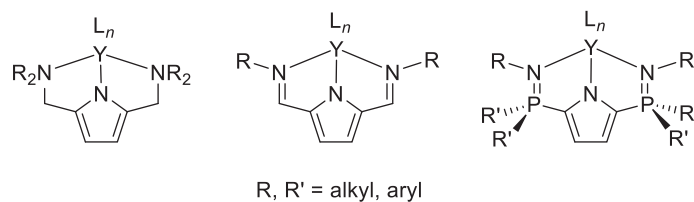


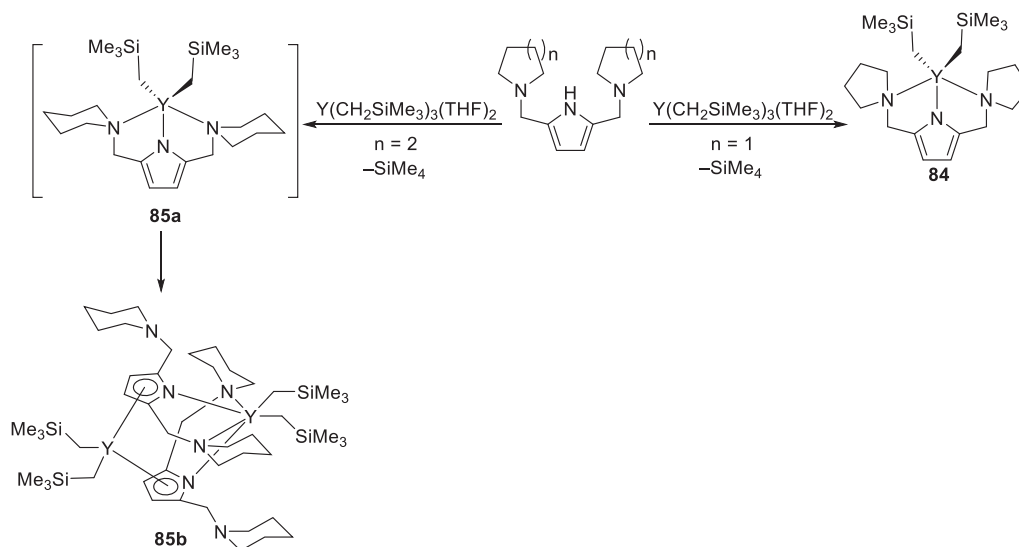
Fig. 14 Generic structures of common pyrrole-based pincer complexes of yttrium.

60 °C, whereas the carbazole analogue, complex (**60**) (*vide supra*) was susceptible to rapid cyclometalative decomposition under ambient conditions (**Fig. 15**).^{70,88} Presumably, the change from a 6-membered to 5-membered chelate ring served to move the phosphinimine substituents further from the metal center, rendering cyclometalation less energetically viable.

4.03.3.3 Monoanionic, Polydentate Ligands

4.03.3.3.1 Indolyl-containing frameworks

Monoanionic indolyl ligands have exhibited a broad range of bonding motifs, including N -bound η^1 and η^3 azaallyl modes, as well as both η^5 and η^6 coordination through the five and six membered rings, respectively (Fig. 16).⁸⁹



Scheme 43 Synthesis of yttrium complexes **84** and **85b**.

The indolyl backbone can also be functionalized to include additional coordinating groups, the most popular of which are substituted aminoalkyl and imine donors (Fig. 17).

Wang et al. have been the main contributors to yttrium indolyl chemistry and have shown the coordinative and chemical versatility of complexes containing imine and aminomethyl functionalized indolyl ligands.^{90–94} For example, reaction of (2-(2,6-*i*-Pr₂C₆H₃N=CH)C₈H₅NH), **In**^a, with Y(CH₂SiMe₃)₃(THF)₂ afforded the monometallic complex [$\{2-(2,6-*i*-Pr_2C_6H_3N=CH)$

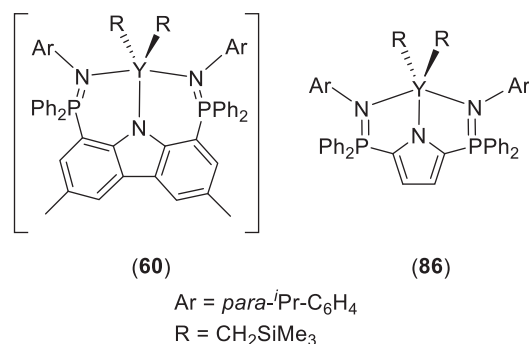


Fig. 15 Bisphosphinimine carbazole and pyrrole stabilized yttrium complexes (**60**) and (**86**).

C₈H₅N₂Y(CH₂SiMe₃)(THF)]₂, (**87**), (Scheme 44), which was capable of polymerizing isoprene with an impressive 98% 1,4-*cis* selectivity, though co-catalysts Al^{*i*}Bu₃ and [Ph₃C][B(C₆F₅)₄] were required and a strong dependence on the AlR₃:catalyst

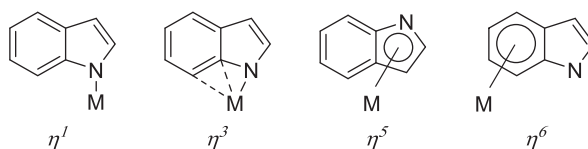


Fig. 16 Coordination modes possible for indolyl ligands to a single metal.

ratio (10:1) was established to be key for optimal performance.⁹⁰ Attempts to prepare a hydride species, by reaction of complex (87) with phenylsilane afforded $[Y\{2-(2,6\text{-}i\text{Pr}_2\text{C}_6\text{H}_3\text{N}=\text{CH})\text{C}_8\text{H}_5\text{N}\}\{\mu\text{-}\eta^6\text{:}\eta^1\text{:}\eta^1\text{-}2-(2,6\text{-}i\text{Pr}_2\text{C}_6\text{H}_3\text{N}-\text{CH}_2)\text{C}_8\text{H}_5\text{N}\}]_2$, (88), which displays a novel $\mu\text{-}\eta^6\text{:}\eta^1\text{:}\eta^1$ coordination mode (Scheme 44). While no evidence was obtained for a hydride species, H⁻ migration from yttrium to the imine carbon is a plausible route for generating the alkylamine pyrrole ligands contained in the product.

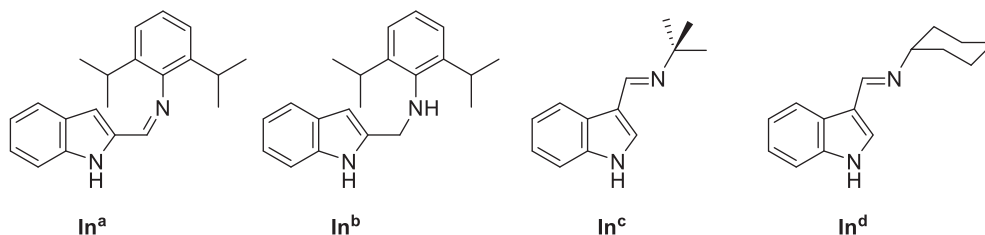
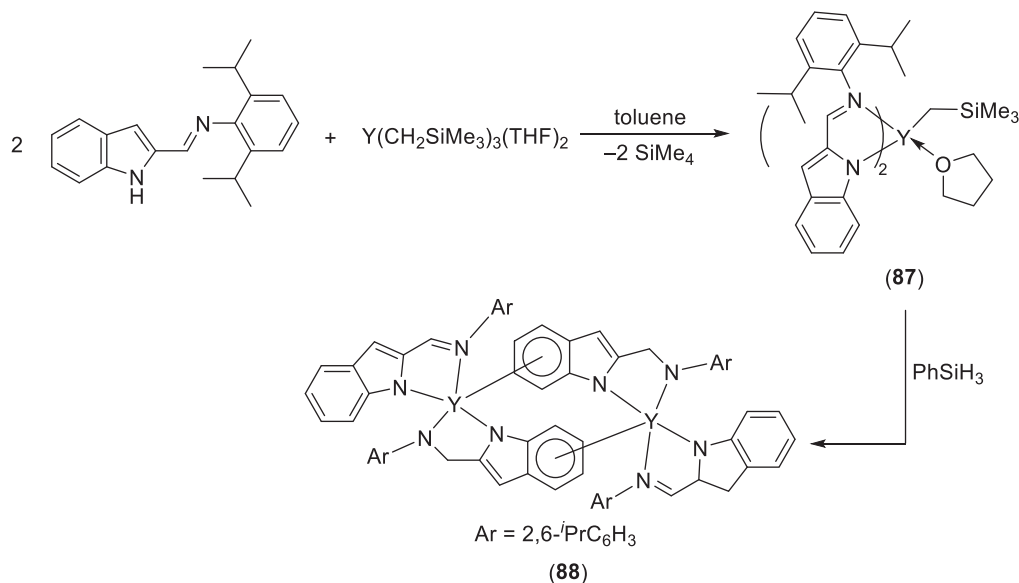


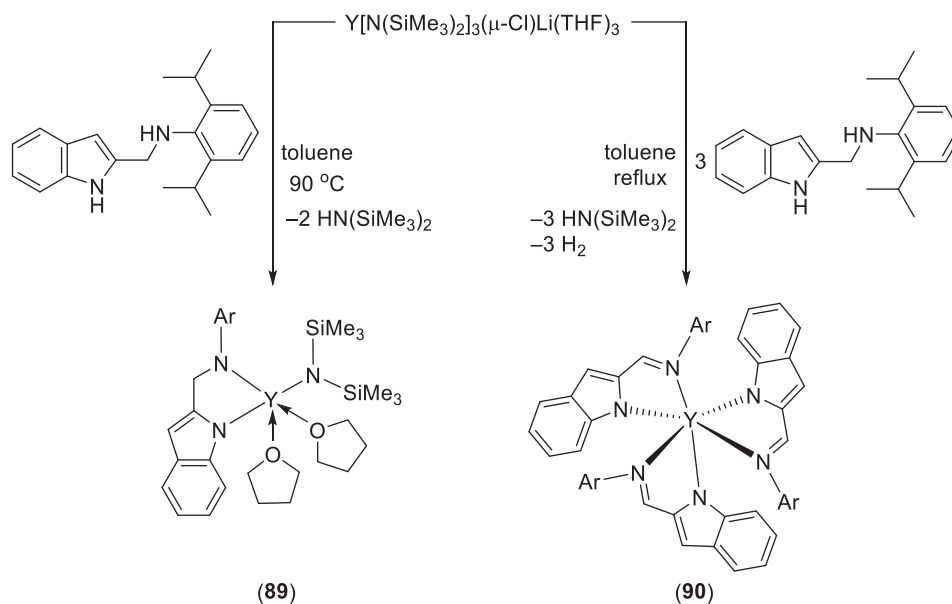
Fig. 17 Derivatized indolyl ligands.

Heating of $2-(2,6\text{-}i\text{Pr}_2\text{C}_6\text{H}_3\text{NHCH}_2)\text{C}_8\text{H}_5\text{NH}$, **In^b**, with $[Y(\text{N}(\text{SiMe}_3)_2)_3(\mu\text{-Cl})\text{Li}(\text{THF})_3]$ at 90 °C in toluene formed the expected monoamido product $[\{2-(2,6\text{-}i\text{Pr}_2\text{C}_6\text{H}_3\text{NCH}_2)\text{C}_8\text{H}_5\text{N}\}Y(\text{N}(\text{SiMe}_3)_2)(\text{THF})_2]$, (89), (Scheme 45, left) in 62% yield.⁹⁴ However, when the reactant stoichiometry was changed and the reaction conducted in refluxing toluene for 24 h, the trisiminopyrrole complex $[Y\{2-(2,6\text{-}i\text{Pr}_2\text{C}_6\text{H}_3\text{N}=\text{CH})\text{C}_8\text{H}_5\text{N}\}]_3$, (90), prevailed (Scheme 45, right). As such work demonstrates, amide to imine conversion, and vice versa, is often a facile process which has the potential to be intentionally invoked. Complex (89) is a potent catalyst for intramolecular hydroamination reactions with high turnover frequencies obtained with a 2–5% catalyst loading.⁹⁴ Catalyst performance was superior for substrates bearing phenyl groups β to nitrogen, as well as for those that formed 5-membered rings.



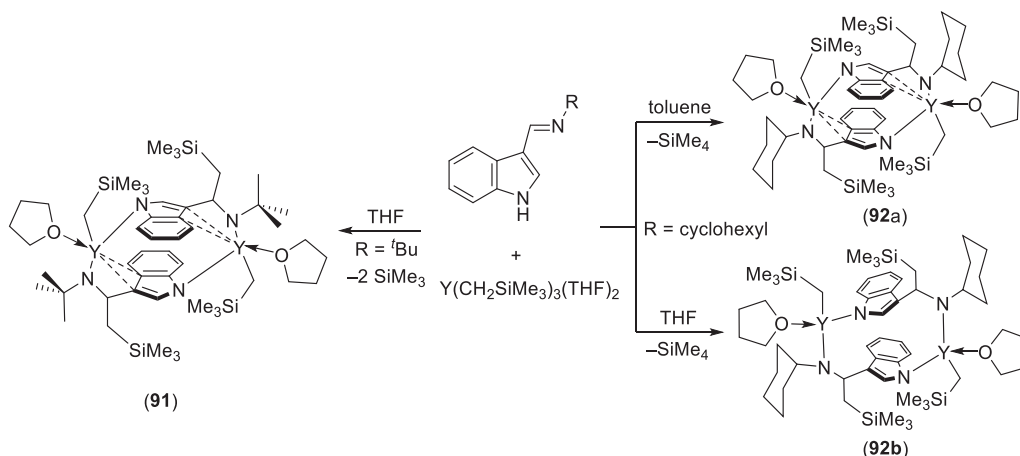
Scheme 44 Synthesis of bisindolyl complex (87); and reaction of (87) with PhSiH_3 to form dinuclear (88).

Reaction of the alkyl substituted iminoindolyl ligands $3-(\text{tBuN}=\text{CH})\text{C}_8\text{H}_5\text{NH}$, **In^c**, and $3-(\text{CyN}=\text{CH})\text{C}_8\text{H}_5\text{NH}$, **In^d**, with $Y(\text{CH}_2\text{SiMe}_3)_3(\text{THF})_2$ generated the unusual dinuclear species $[\{\mu\text{-}\eta^2\text{:}\eta^1\text{:}\eta^1\text{-}3-(\text{tBuNCH}(\text{CH}_2\text{SiMe}_3))\text{C}_8\text{H}_5\text{N}\}Y(\text{CH}_2\text{SiMe}_3)(\text{THF})_2]$, (91) and $[\{\mu\text{-}\eta^2\text{:}\eta^1\text{:}\eta^1\text{-}3-(\text{CyNCH}(\text{CH}_2\text{SiMe}_3))\text{C}_8\text{H}_5\text{N}\}Y(\text{CH}_2\text{SiMe}_3)(\text{THF})_2]$, (92a), respectively (Scheme 46). In both of these complexes the two six membered rings on the indolyl ligands are stacked parallel and oriented in opposite directions from each other.^{91,92} Notably, the new complexes bear derivatized ligands resulting from CH_2SiMe_3 migration from yttrium to the imine carbon. Although rare, metal to ligand transfer of CH_2SiMe_3 groups to pyrimidine⁹⁵ and terpyridine⁹⁶ moieties has been reported for lutetium complexes supported by nitrogenous ancillary ligands. The resulting dianionic ligands each



Scheme 45 Synthesis of amide and imine indolyl yttrium complexes (89) and (90).

bridge two yttrium centers *via* a unique $\mu\text{-}\eta^2\text{:}\eta^1\text{:}\eta^1$ motif. In addition, the binding mode observed for In^{d} is solvent dependent; the $\mu\text{-}\eta^2$ interaction between the π -system of the indolyl backbone and the metal center is only observed when the reaction is performed in toluene. When the aforementioned reaction was completed in THF, $[\{\mu\text{-}\eta^1\text{:}\eta^1\text{-}3\text{-}(\text{C}_8\text{H}_5\text{N})\}\text{Y}(\text{CH}_2\text{SiMe}_3)(\text{THF})]_2$, (92b), which has the six membered indolyl rings facing in the same direction was formed. Both complexes (92a) and (92b) catalyzed the polymerization of isoprene polymerization with high 1,4-*trans* regioselectivity (75–98%) when Al^iBu_3 and $[\text{Ph}_3\text{C}][\text{B}(\text{C}_6\text{F}_5)_4]$ were used as co-catalysts. Significantly, when the substrate: catalyst ratio was increased a proportional increase in the number average molecular weight (M_n) of the polymer was observed. Changing the stoichiometry of the reaction between In^{c} and $\text{Y}(\text{CH}_2\text{SiMe}_3)_3(\text{THF})_2$ to a 4:3 ratio resulted in the trinuclear species $[\text{Y}_3\{\mu\text{-}\eta^1\text{:}\eta^2\text{:}\eta^1\text{-}3\text{-}(\text{C}_8\text{H}_5\text{N})\}_4(\text{CH}_2\text{SiMe}_3)(\text{THF})_5]$, (93), which features unique $\mu\text{-}\eta^1\text{:}\eta^2\text{:}\eta^1$ bonding wherein each indolyl is η^2 bound to a single yttrium center through the 2 and 3 carbons and η^1 bound *via* the pendant nitrogen donor. The indolyl nitrogen is bonded in an η^1 fashion to a separate metal center.



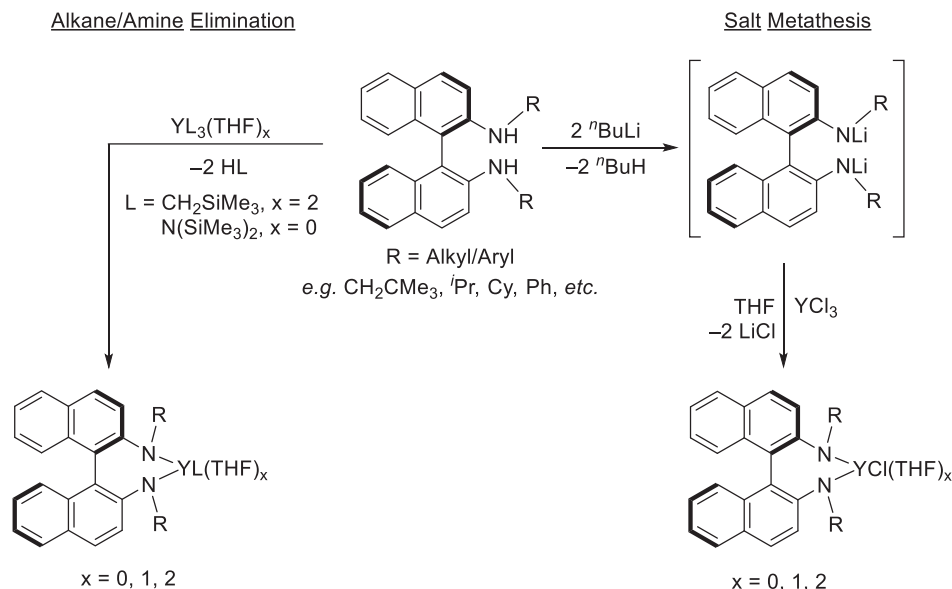
Scheme 46 Synthesis of complexes (91) and (92).

4.03.4 Dianionic Ligands

4.03.4.1 Dianionic, Bidentate N,N Donors

4.03.4.1.1 Binaphthylamido ligands

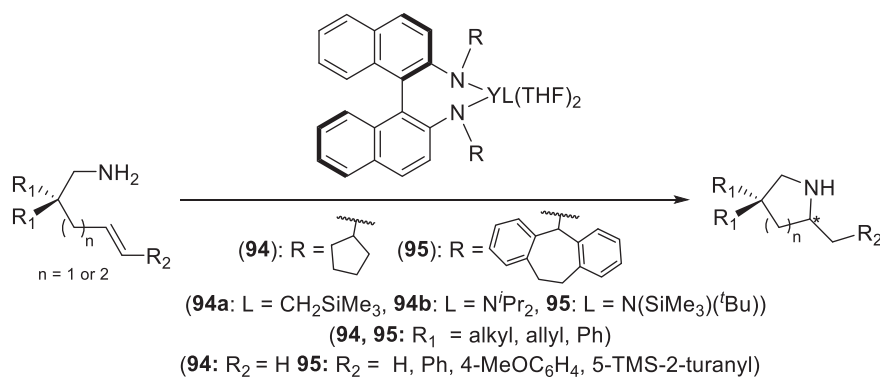
Binaphthyl ligands are commonly used as chiral directing groups in asymmetric catalysis.^{97,98} Starting from binaphthol, the coordinating heteroatom can be readily converted to a phosphine, amine/amide or alkylhalide, thereby providing access to a plethora of ligands with different donor groups.⁹⁷ Both *R* and *S* enantiomers can be synthesized, and their steric bulk renders such moieties attractive for isoselective reactions.



Scheme 47 Common synthetic strategies for binaphthylamido ligand coordination.

As dianionic, bulky, bidentate ligands, binaphthylamides are well suited to stabilizing yttrium complexes. Synthetic strategies for forming yttrium binaphthylamido complexes follow classic salt metathesis or elimination routes (Scheme 47).^{99,100}

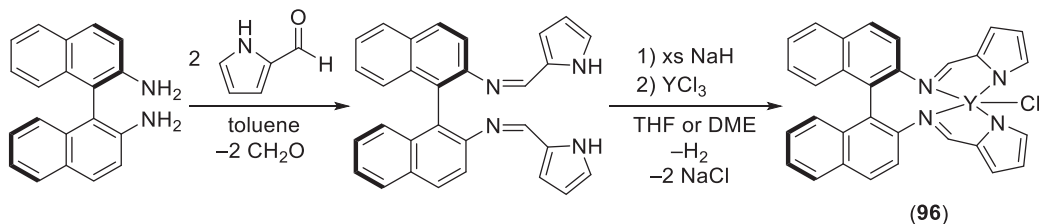
Applications for yttrium binaphthylamido complexes have focused primarily on their use for catalytic asymmetric hydroamination reactions that form chiral heterocycles. Both Collin et al. and Living house and colleagues have shown high *ee*'s and percent conversions using sterically demanding binaphthylamido yttrium catalysts for the intramolecular cyclization of aminoalkenes (Scheme 48).^{99,101} Specifically, Collin and co-workers have utilized cyclopentyl nitrogen substituents to form complexes $\{(R)\text{-BINAP-(NC}_5\text{H}_9)_2\}YL(THF)_2$, (**94a**: $L = CH_2SiMe_3$, **94b**: $L = N^iPr_2$, **95**: $L = N(SiMe_3)(\textit{i}Bu)$), that catalyze the intramolecular hydroamination of terminal aminoalkenes with conversions and *ee*'s of up to 100% and 81%, respectively.⁹⁹ The closely related dibenzosuberylyl analogue $\{(R)\text{-}$



Scheme 48 Intramolecular hydroamination catalyzed by complexes (**94**) and (**95**).

BINAP-(NC₁₅H₁₃)₂Y(N(SiMe₃)₂(^tBu)) (THF)₂, (95), catalyzes hydroamination of both terminal and internal aminoalkenes with >95% conversions and up to 87% *ee*, but this more sterically demanding catalyst requires multiday reaction times for most substrates.¹⁰¹

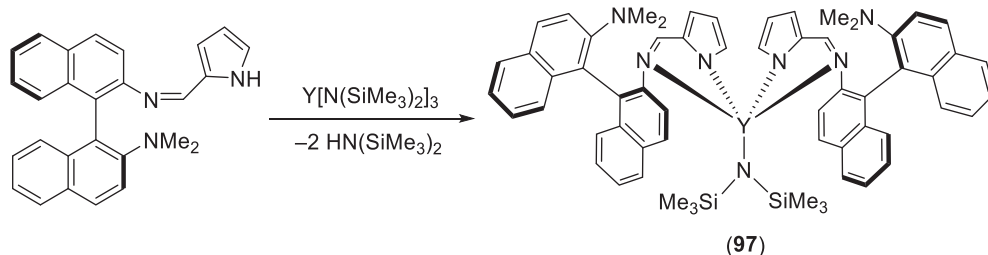
Zi and colleagues developed a dianionic, tetradentate bisimino pyrrole scaffold that features a binaphthyl core. This ligand was successfully used to generate the yttrium chloride complex [$\{(R)\text{-BINAP-}(N=CH(C_4H_3N))_2\}YCl$], (96) (Scheme 49).¹⁰² When applied to intramolecular hydroamination only modest *ee*'s (2.2–22%) were reported, but the reaction proceeded to >90% conver-



Scheme 49 Synthesis of complex (96).

sion in 6 h at 60 °C in benzene-*d*₆ solution. The group also investigated the complex's ability to catalyze methyl methacrylate polymerization was also investigated, but only limited conversions (4.5–7.5%) and modest syndiotactic (MR= 29%) selectivity were observed under the conditions examined.

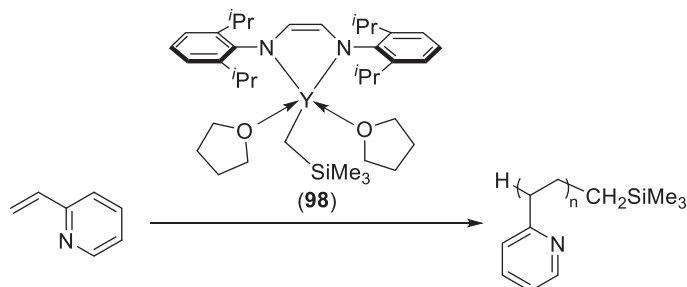
Two equivalents of the monosubstituted version of their ligand bind to yttrium in a bidentate fashion wherein the dimethylamino moieties do not coordinate to the metal center (Scheme 50).¹⁰³ Accordingly, it is not surprising that [$\{(S)\text{-}(NMe_2)\text{BINAP-}(N=CH(C_4H_3N))_2\}_2Y(N(SiMe_3)_2)$], (97), fails to impart substantial enantioselectivity (25–60%) when used as a catalyst for intramolecular hydroamination reactions.



Scheme 50 Preparation of the asymmetric binaphthyl-supported yttrium complex (97).

4.03.4.1.2 Diamide ligands

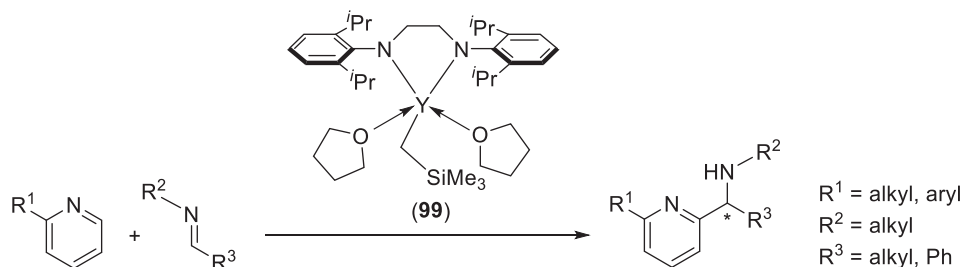
Bidentate ligands that coordinate through two amido functionalities have been utilized to generate a number of organometallic yttrium complexes over the past decade. One such well-studied species, [$\{(2,6\text{-}^i\text{Pr}_2\text{C}_6\text{H}_3)\text{NCH=CHN}(2,6\text{-}^i\text{Pr}_2\text{C}_6\text{H}_3)\}_2Y(\text{CH}_2\text{Si-}$



Scheme 51 Polymerization of 2-vinylpyridine by complex (98).

Me₃)(THF)₂, (98), which was reported by Mashima et al. can catalyze the polymerization of 2-vinylpyridine in toluene at ambient temperature with isotacticity as high as [*mmmm*] = 95% and yields up to 85% in only 15 min (Scheme 51).¹⁰⁴

When substituted pyridine and alkyne additives were introduced to the polymerization reaction mixture C–H bond activation of these substrates resulted in end functionalization of the poly-2-vinylpyridine product.¹⁰⁴ The same group has also prepared the organoyttrium complex [$\{(2,6\text{-}i\text{Pr}_2\text{C}_6\text{H}_3)\text{NCH}_2\text{CH}_2\text{N}(2,6\text{-}i\text{Pr}_2\text{C}_6\text{H}_3)\}\text{Y}(\text{CH}_2\text{SiMe}_3)(\text{THF})_2$], (**99**), which is stabilized by a saturated diarylethylenediamido ligand.¹⁰⁵ This species effectively catalyzes the addition of imines to *ortho*-substituted pyridines, with exclusive regioselectivity for the remaining *ortho* site (**Scheme 52**). Ligand alteration revealed that when a chiral group is incorporated



Scheme 52 Regio- and stereoselective aminoalkylation of substituted pyridines.

into the backbone the reaction can be performed stereoselectively. For example, installation of phenyl groups on the backbone carbons in combination with 2-MeOC₆H₄ moieties on the flanking nitrogen atoms provided high enantiomeric excess (*ee* = 97%), but with low yields (20%).¹⁰⁵

4.03.5 Concluding Remarks

The past decade has yielded many new multidentate nitrogen ligand sets that are capable of supporting discrete yttrium complexes. As methodologies for preparing useful yttrium starting materials, and protocols for the subsequent installation of ligand scaffolds, have become more robust and established, exploration into the reactivity of complexes bearing previously reported frameworks have led to unusual complexes and systems capable of mediating various chemical transformations. Notably, extremely high activities and selectivities have been demonstrated in the catalytic polymerization of lactones and olefins. Many of these catalyst systems, however, still rely on cationic “activators” to achieve these impressive results. Given the ongoing efforts to develop increasingly sophisticated yttrium species supported by nitrogen donors, there is little doubt that such complexes will continue to evolve and play an important role in the development of new stoichiometric and catalytic reactions for the foreseeable future.

References

- O’Keefe, B. J.; Hillmyer, M. A.; Tolman, W. B. *J. Chem. Soc. Dalton Trans.* **2001**, 30, 2215–2224.
- Hou, Z.; Wakatsuki, Y. *Coord. Chem. Rev.* **2002**, 231, 1–22.
- Pagis, C.; Ferbinteanu, M.; Rothenberg, G.; Tanase, S. *ACS Catal.* **2016**, 6, 6063–6072.
- Day, B. M.; Guo, F.-S.; Layfield, R. A. *Acc. Chem. Res.* **2018**, 51, 1880–1889.
- Hewitt, S. H.; Butler, S. J. *Chem. Commun.* **2018**, 54, 6635–6647.
- Nief, F. In *Handbook on the Physics and Chemistry of Rare Earths*, vol. 40; Elsevier, 2010; pp 241–300. Chapter 246.
- Woen, D. H.; Evans, W. J. In *Handbook on the Physics and Chemistry of Rare Earths*; Bünzli, J.-C. G., Pecharsky, V. K., Eds.; Vol. 50; Elsevier, 2016; pp 337–394. Chapter 293.
- Anwander, R.; Dolg, M.; Edelmann, F. T. *Chem. Soc. Rev.* **2017**, 46, 6697–6709.
- So, Y.-M.; Leung, W.-H. *Coord. Chem. Rev.* **2017**, 340, 172–197.
- Nief, F. *Dalton Trans.* **2010**, 39, 6589–6598.
- Garcia, J. *Eur. J. Inorg. Chem.* **2012**, 2012, 4550–4563.
- Hänninen, M.; Zamora, M. T.; Hayes, P. G. *The Privileged Pincer-Metal Platform: Coordination Chemistry & Applications*; vol. 54; Springer, 2016; pp 93–177.
- Cotton, S. *Polyhedron* **1996**, 15, 3665.
- McCleverty, J. A.; Meyer, T. J. *Comprehensive Coordination Chemistry II: From Biology to Nanotechnology*, 1st ed; Elsevier: Amsterdam, 2003.
- Mishra, S. *Coord. Chem. Rev.* **2008**, 252, 1996–2025.
- Piers, W. E.; Emslie, D. J. H. *Coord. Chem. Rev.* **2002**, 233–234, 131–155.
- Fisher, K. J. In *Comprehensive Coordination Chemistry II*; McCleverty, J. A., Meyer, T. J., Eds.; Pergamon: Oxford, 2003; pp 1–29. Chapter 4.1.
- Burger, B. J.; Bercaw, J. E. *Am. Chem. Soc.* **1987**, 357, 79–115.
- Emslie, D. J. H.; Piers, W. E.; Parvez, M.; McDonald, R. *Organometallics* **2002**, 21, 4226–4240.
- Bourget-Merle, L.; Lappert, M. F.; Severn, J. R. *Chem. Rev.* **2002**, 102, 3031–3066.
- Kenward, A. L.; Piers, W. E.; Parvez, M. *Organometallics* **2009**, 28, 3012–3020.
- Liddle, S. T.; Arnold, P. L. *Dalton Trans.* **2007**, 36, 3305–3313.
- Wei, X.; Cheng, Y.; Hitchcock, P. B.; Lappert, M. F. *Dalton Trans.* **2008**, 5235–5246.
- Hayes, P. G. *Synthesis, Structure and Reactivity of β -Diketiminato Supported Organoscandium Cations*, University of Calgary, 2004.
- Hänninen, M. M.; Zamora, M. T.; Hayes, P. G. *Top. Organomet. Chem.* **2016**, 54, 93–177.
- Li, D.; Li, S.; Cui, D.; Zhang, X. *Organometallics* **2010**, 29, 2186–2193.

27. Li, L.; Wu, C.; Liu, D.; Li, S.; Cui, D. *Organometallics* **2013**, *32*, 3203–3209.
28. Mou, Z.; Zhuang, Q.; Xie, H.; Luo, Y.; Cui, D. *Dalton Trans.* **2018**, *47*, 14985–14991.
29. Shen, X.; Xue, M.; Jiao, R.; Ma, Y.; Zhang, Y.; Shen, Q. *Organometallics* **2012**, *31*, 6222–6230.
30. Duchateau, R.; van Wee, C. T.; Meetsma, A.; Teuben, J. H. *J. Am. Chem. Soc.* **1993**, *115*, 4931–4932.
31. Bailey, P. J.; Pace, S. *Coord. Chem. Rev.* **2001**, *214*, 91–141.
32. Ge, S.; Meetsma, A.; Hessen, B. *Organometallics* **2008**, *27*, 3131–3135.
33. Zhang, L.; Nishiura, M.; Yuki, M.; Luo, Y.; Hou, Z. *Angew. Chem. Int. Ed.* **2008**, *47*, 2642–2645.
34. Nagae, H.; Kundu, A.; Tsurugi, H.; Mashima, K. *Organometallics* **2017**, *36*, 3061–3067.
35. Bochkarev, M. N.; Maleev, A. A.; Balashova, T. V.; Fukin, G. K.; Baranov, E. V.; Efimova, Y. A.; Petrov, B. I.; Ilichev, V. A. *Inorg. Chim. Acta* **2008**, *361*, 2533–2539.
36. Cheng, J.; Hou, Z. *Chem. Commun.* **2012**, *48*, 814–816.
37. Hamidi, S.; Jende, L. N.; Martin Dietrich, H.; Maichle-Moessmer, C.; Tornroos, K. W.; Deacon, G. B.; Junk, P. C.; Anwender, R. *Organometallics* **2013**, *32*, 1209–1223.
38. Jende, L. N.; Maichle-Moessmer, C.; Anwender, R. *J. Organomet. Chem.* **2018**, *857*, 138–144.
39. Luo, Y.; Fan, S.; Yang, J.; Fang, J.; Xu, P. *Dalton Trans.* **2011**, *40*, 3053–3059.
40. Wang, Y.; Luo, Y.; Chen, J.; Xue, H.; Liang, H. *New J. Chem.* **2012**, *36*, 933–940.
41. Hong, J.; Li, Z.; Chen, Z.; Weng, L.; Zhou, X.; Zhang, L. *Dalton Trans.* **2016**, *45*, 6641–6649.
42. Yu, X.; You, Q.; Zhou, X.; Zhang, L. *ACS Catal.* **2018**, *8*, 4465–4472.
43. Yu, X.; Li, M.; Hong, J.; Zhou, X.; Zhang, L. *Chem. A Eur. J.* **2019**, *25*, 2569–2576.
44. Wang, J.; Sun, H.; Yao, Y.; Zhang, Y.; Shen, Q. *Polyhedron* **2008**, *27*, 1977–1982.
45. Skvortsov, G. G.; Tolpygin, A. O.; Fukin, G. K.; Cherkasov, A. V.; Trifonov, A. A. *Eur. J. Inorg. Chem.* **2010**, 1655–1662.
46. Tolpygin, A. O.; Shayrin, A. S.; Cherkasov, A. V.; Fukin, G. K.; Trifonov, A. A. *Organometallics* **2012**, *31*, 5405–5413.
47. Tolpygin, A. O.; Skvortsov, G. G.; Cherkasov, A. V.; Fukin, G. K.; Glukhova, T. A.; Trifonov, A. A. *Eur. J. Inorg. Chem.* **2013**, *2013*, 6009–6018.
48. Tolpygin, A. O.; Cherkasov, A. V.; Fukin, G. K.; Trifonov, A. A. *Russ. Chem. Bull.* **2014**, *63*, 2299–2304.
49. Yakovenko, M. V.; Udilova, N. Y.; Glukhova, T. A.; Cherkasov, A. V.; Fukin, G. K.; Trifonov, A. A. *New J. Chem.* **2015**, *39*, 1083–1093.
50. Yakovenko, M. V.; Cherkasov, A. V.; Fukin, G. K.; Trifonov, A. A. *Russ. Chem. Bull.* **2013**, *62*, 1772–1776.
51. Benndorf, P.; Kratsch, J.; Hartenstein, L.; Preuss, C. M.; Roesky, P. W. *Chem. A Eur. J.* **2012**, *18*, 14454–14463.
52. Brunner, T. S.; Benndorf, P.; Gamer, M. T.; Knoefel, N.; Gugau, K.; Roesky, P. W. *Organometallics* **2016**, *35*, 3474–3487.
53. Zhang, Z.; Zhang, L.; Li, Y.; Hong, L.; Chen, Z.; Zhou, X. *Inorg. Chem.* **2010**, *49*, 5715–5722.
54. Lyubov, D. M.; Fukin, G. K.; Trifonov, A. A. *Inorg. Chem.* **2007**, *46*, 11450–11456.
55. Ajellal, N.; Lyubov, D. M.; Sinenkov, M. A.; Fukin, G. K.; Cherkasov, A. V.; Thomas, C. M.; Carpentier, J.-F.; Trifonov, A. A. *Chem. A Eur. J.* **2008**, *14*, 5440–5448.
56. Lyubov, D. M.; Bubnov, A. M.; Fukin, G. K.; Dolgushin, F. M.; Antipin, M. Y.; Pelce, O.; Schappacher, M.; Guillaume, S. M.; Trifonov, A. A. *Eur. J. Inorg. Chem.* **2008**, 2090–2098.
57. Nie, K.; Liu, C.; Zhang, Y.; Yao, Y. *Sci. China Chem.* **2015**, *58*, 1451–1460.
58. Bérubé, C. D.; Yazdanbakhsh, M.; Gambarotta, S.; Yap, G. P. A. *Organometallics* **2003**, *22*, 3742–3747.
59. Zhou, S.; Yin, C.; Wang, H.; Zhu, X.; Yang, G.; Wang, S. *Inorg. Chem. Commun.* **2011**, *14*, 1196–1200.
60. Kaneko, H.; Dietrich, H. M.; Schadle, C.; Maichle-Moessmer, C.; Tsurugi, H.; Tornroos, K. W.; Mashima, K.; Anwender, R. *Organometallics* **2013**, *32*, 1199–1208.
61. Li, Q.; Zhou, S.; Wang, S.; Zhu, X.; Zhang, L.; Feng, Z.; Guo, L.; Wang, F.; Wei, Y. *Dalton Trans.* **2013**, *42*, 2861–2869.
62. Wang, W.; Wang, X.; Zhou, S.; Xu, X.; Du, J.; Zhang, L.; Mu, X.; Wei, Y.; Zhu, X.; Wang, S. *Inorg. Chem.* **2018**, *57*, 10390–10400.
63. Zou, J.; Berg, D. J.; Stuart, D.; McDonald, R.; Twamley, B. *Organometallics* **2011**, *30*, 4958–4967.
64. Johnson, K. R. D.; Hayes, P. G. *Organometallics* **2009**, *28*, 6352–6361.
65. Inoue, M.; Nakada, M. *Angew. Chem. Int. Ed.* **2006**, *45*, 252–255.
66. Inoue, M.; Suzuki, T.; Nakada, M. *J. Am. Chem. Soc.* **2003**, *125*, 1140–1141.
67. Matsumoto, K.; Suzuki, K.; Tsukuda, T.; Tsubomura, T. *Inorg. Chem.* **2010**, *49*, 4717–4719.
68. Wang, L.; Cui, D.; Hou, Z.; Li, W.; Li, Y. *Organometallics* **2011**, *30*, 760–767.
69. Wong, E. W. Y.; Emslie, D. J. H. *Dalton Trans.* **2015**, *44*, 11601–11612.
70. Johnson, K. R. D.; Hayes, P. G. *Inorg. Chim. Acta* **2014**, *422*, 209–217.
71. Pettinari, C.; Pettinari, R.; Marchetti, F.; Pérez, P. J., Ed. Academic Press: 2016; vol. 65, pp 175–260.
72. Muñoz-Molina, J. M.; Belderrain, T. R.; Pérez, P. J. *Coord. Chem. Rev.* **2019**, *390*, 171–189.
73. Cheng, J.; Saliu, K.; Kiel, G. Y.; Ferguson, M. J.; McDonald, R.; Takats, J. *Angew. Chem. Int. Ed.* **2008**, *47*, 4910–4913.
74. Cheng, J.; Saliu, K.; Ferguson, M. J.; McDonald, R.; Takats, J. *J. Organomet. Chem.* **2010**, *695*, 2696–2702.
75. Yi, W.; Zhang, J.; Zhang, F.; Zhang, Y.; Chen, Z.; Zhou, X. *Chem. A Eur. J.* **2013**, *19* (36), 11975–11983.
76. Cheng, J.-H.; Ferguson, M. J.; Takats, J. *J. Am. Chem. Soc.* **2010**, *132*, 2–3.
77. Littlaboe, R.; Zimmermann, M.; Saliu, K.; Takats, J.; Toernroos, K. W.; Anwender, R. *Angew. Chem. Int. Ed.* **2008**, *47*, 9560–9564.
78. Zimmermann, M.; Takats, J.; Kiel, G.; Toernroos, K. W.; Anwender, R. *Chem. Commun.* **2008**, 612–614.
79. Schaedle, C.; Schaedle, D.; Eichele, K.; Anwender, R. *Angew. Chem. Int. Ed.* **2013**, *52*, 13238–13242.
80. Schaedle, D.; Meermann-Zimmermann, M.; Schaedle, C.; Maichle-Moessmer, C.; Anwender, R. *Eur. J. Inorg. Chem.* **2015**, *2015*, 1334–1339.
81. Yi, W.; Zhang, J.; Li, M.; Chen, Z.; Zhou, X. *Inorg. Chem.* **2011**, *50*, 11813–11824.
82. Yi, W.; Zhang, J.; Chen, Z.; Zhou, X. *Organometallics* **2012**, *31*, 7213–7221.
83. Yi, W.; Zhang, J.; Hong, L.; Chen, Z.; Zhou, X. *Organometallics* **2011**, *30*, 5809–5814.
84. Yi, W.; Zhang, J.; Chen, Z.; Zhou, X. *Inorg. Chem.* **2012**, *51*, 10631–10638.
85. Yi, W.; Huang, S.; Zhang, J.; Chen, Z.; Zhou, X. *Organometallics* **2013**, *32*, 5409–5415.
86. Yi, W.; Zhang, J.; Huang, S.; Weng, L.; Zhou, X. *Chem. A Eur. J.* **2014**, *20*, 867–876.
87. Meyer, N.; Kuzdrowska, M.; Roesky, P. W. *Eur. J. Inorg. Chem.* **2008**, 1475–1479.
88. Zamora, M. T.; Johnson, K. R. D.; Hanninen, M. M.; Hayes, P. G. *Dalton Trans.* **2014**, *43*, 10739–10750.
89. Evans, W. J.; Brady, J. C.; Ziller, J. W. *Inorg. Chem.* **2002**, *41*, 3340–3346.
90. Zhang, G.; Wang, S.; Zhou, S.; Wei, Y.; Guo, L.; Zhu, X.; Zhang, L.; Gu, X.; Mu, X. *Organometallics* **2015**, *34*, 4251–4261.
91. Zhang, G.; Wei, Y.; Guo, L.; Zhu, X.; Wang, S.; Zhou, S.; Mu, X. *Chem. A Eur. J.* **2015**, *21*, 2519–2526.
92. Zhang, G.; Deng, B.; Wang, S.; Wei, Y.; Zhou, S.; Zhu, X.; Huang, Z.; Mu, X. *Dalton Trans.* **2016**, *45*, 15445–15456.
93. Zhang, G.; Wang, S.; Zhu, X.; Zhou, S.; Wei, Y. *Organometallics* **2017**, *36*, 3812–3822.
94. Feng, Z.; Wei, Y.; Zhou, S.; Zhang, G.; Zhu, X.; Guo, L.; Wang, S.; Mu, X. *Dalton Trans.* **2015**, *44*, 20502–20513.
95. Johnson, K. R. D.; Hayes, P. G. *Organometallics* **2013**, *32*, 4046–4049.
96. Jantunen, K. C.; Scott, B. L.; Hay, P. J.; Gordon, J. C.; Kiplinger, J. L. *J. Am. Chem. Soc.* **2006**, *128*, 6322–6323.
97. Shockravi, A.; Javadi, A.; Abouzari-Lotf, E. *RSC Adv.* **2013**, *3*, 6717–6746.
98. Misra, A.; Dwivedi, J.; Kishore, D. *Synth. Commun.* **2017**, *47*, 497–535.

99. Aillaud, I.; Collin, J.; Hannedouche, J.; Schulz, E.; Trifonov, A. *Tetrahedron Lett.* **2010**, *51*, 4742–4745.
100. Queffelec, C.; Boeda, F.; Pouilhes, A.; Meddour, A.; Kouklovsky, C. *ChemCatChem* **2011**, *3*, 122–126.
101. Huynh, K.; Livinghouse, T.; Lovick, H. M. *Synlett* **2014**, *25*, 1721–1724, 4 pp.
102. Xiang, L.; Wang, Q.; Song, H.; Zi, G. *Organometallics* **2007**, *26*, 5323–5329.
103. Zi, G.; Xiang, L.; Song, H. *Organometallics* **2008**, *27*, 1242–1246.
104. Kaneko, H.; Nagae, H.; Tsurugi, H.; Mashima, K. *J. Am. Chem. Soc.* **2011**, *133*, 19626–19629.
105. Kundu, A.; Inoue, M.; Nagae, H.; Tsurugi, H.; Mashima, K. *J. Am. Chem. Soc.* **2018**, *140*, 7332–7342.